

TERMINATOR: Learning Optimal Exit Points for Early Stopping in Chain-of-Thought Reasoning

Alliot Nagle¹ Jakhongir Saydaliev² Dhia Garbaya^{2,3} Michael Gastpar^{†,2}
Ashok Vardhan Makkuva^{†,4} Hyeji Kim^{†,1}

Abstract

Large Reasoning Models (LRMs) achieve impressive performance on complex reasoning tasks via Chain-of-Thought (CoT) reasoning, which enables them to generate intermediate thinking tokens before arriving at the final answer. However, LRMs often suffer from significant *overthinking*, spending excessive compute time even after the answer is generated early on. Prior work has identified the existence of an optimal reasoning length such that truncating reasoning at this point significantly shortens CoT outputs with virtually no change in performance. However, determining optimal CoT lengths for practical datasets is highly non-trivial as they are fully task and model-dependent. In this paper, we precisely address this and design TERMINATOR, an early-exit strategy for LRMs at inference to mitigate overthinking. The central idea underpinning TERMINATOR is that the first arrival of an LRM’s final answer is often predictable, and we leverage these first answer positions to create a novel dataset of optimal reasoning lengths to train TERMINATOR. Powered by this approach, TERMINATOR achieves significant reductions in CoT lengths of 14%–55% on average across four challenging practical datasets: MATH-500, AIME 2025, HumanEval, and GPQA, whilst outperforming current state-of-the-art methods.

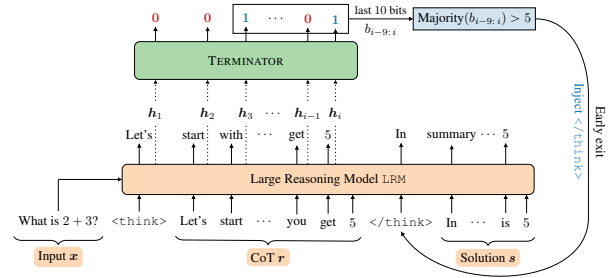


Figure 1. Early stopping via TERMINATOR. TERMINATOR is a binary probe classifier that predicts whether to exit or not at every CoT token. Once the majority of prediction bits within a window (10 here) are 1, `</think>` is injected into the LRM’s token stream to stop thinking (Sec. 4).

performance gains across many challenging tasks (OpenAI, 2024). However, this improvement does not come for free, as an LRM will generate thousands of additional thinking tokens to solve a single problem, compared to its non-reasoning counterparts (Guo et al., 2025). Worse yet, LRMs spend a significant amount of their reasoning tokens double-checking their work and exploring different solutions when they have already generated the final answer, that they will eventually settle on, much earlier in the CoT, a phenomenon known as *overthinking* (Luo et al., 2025; Chen et al., 2025). Prior work has shown that the length of a CoT can be reduced by 50% or more on average with little drop in accuracy (Kang et al., 2025a; Zhang et al., 2025b; Yang et al., 2025b), demonstrating the extent to which compute is wasted during LRM inference.

Given that reasoning can be wasteful, a natural question to ask is, *for any given accuracy, does there exist an optimal reasoning length?* Previous works have shown that LRM performance, as a function of reasoning length, gradually increases, peaks, and then decreases, suggesting the existence of an optimal reasoning length (Wu et al., 2025b; Lee et al., 2025). Additionally, some recent works propose novel RL-training algorithms to fine-tune LRMs to produce shorter CoTs (Luo et al., 2025; Lou et al., 2025; Gao et al., 2025; Yi et al., 2025; Shrivastava et al., 2025) and establish the Pareto frontier for those methods, showing that gaps still exist between them (Gao et al., 2025). While these works focus on retraining an LRM, inference-time

1. Introduction

The advent of Large Reasoning Models (LRMs) has proven itself to be a critical next step for Large Language Models (LLMs) to surpass human-level performance. LRMs use test-time compute to “think” through a problem before answering, an approach that has led to significant

¹UT Austin, US ²EPFL, Switzerland ³ENS Paris-Saclay, France
⁴Télécom Paris (IP Paris), France. Correspondence to: Alliot Nagle <acnagle@utexas.edu>.

methods such as DEER (Yang et al., 2025b) enable early termination of reasoning without retraining it. However, for practical tasks none of these methods either determines or utilizes the optimal-length reasoning, which in fact provides the best possible reduction in CoT length.

In this paper, we precisely address this by introducing the novel notion of *hindsight-optimal reasoning length* (Sec. 2.2): given a reasoning task, in hindsight, what is the fewest number of tokens that an LRM needs to generate before providing the same answer it would have provided without shortened reasoning? Namely, we mark the first logical arrival, as opposed to any other occurrence, of the LRM’s final answer as the hindsight-optimal exiting position. Leveraging this notion, we design a novel inference-time early-exit algorithm TERMINATOR that significantly outperforms current state-of-the-art methods in reductions to CoT lengths on challenging practical datasets (Fig. 1). In particular, TERMINATOR capitalizes on the fact that the first arrival of the final answer is (1) marked by a distinctive shift in the LRM’s token-level confidence and token usage distribution, and (2) can be used as a signal to train a binary probe classifier for effective early-exiting during reasoning.

Main Contributions. In summary, we make the following contributions:

- We introduce the novel notion of hindsight-optimal reasoning, using which we show that the first arrival of an LRM’s final answer is marked by observable and meaningful signals (Sec. 3). To the best of our knowledge, this is the first such analysis of its kind.
- We design TERMINATOR, a novel inference-time early-exit algorithm for LRMs that leverages optimal-length CoTs (Sec. 4.2).
- We introduce a robust pipeline for identifying the first arrival of the final answer in CoTs, using which we construct a novel optimal-length CoT dataset (Sec. 4.1).

2. Preliminaries

2.1. Notation

A Large Reasoning Model LRM takes as input the prompt sequence $\mathbf{x} = (x_1, x_2, x_3, \dots, x_L)$ and produces two outputs \mathbf{r} and \mathbf{s} auto-regressively (Fig. 1). Here $\mathbf{r} = (r_1, r_2, r_3, \dots, r_M)$ is the CoT sequence generated during the thinking stage, i.e. $r_i = \text{LRM}(\mathbf{x}, \mathbf{r}_{<i})$ for $i \in [M] \triangleq \{1, \dots, M\}$, and $\mathbf{s} = (s_1, s_2, s_3, \dots, s_N)$ is the solution that summarizes this CoT and contains a final answer $\hat{\mathbf{a}}$, which could be a single numerical answer, a

math expression, code, a multiple-choice option, etc. Here $s_j = \text{LRM}(\mathbf{x}, \mathbf{r}, \mathbf{s}_{<j})$ for $j \in [N]$. Note that the final answer $\hat{\mathbf{a}}$ is separate from the ground-truth answer \mathbf{a} ; they may or may not be in agreement with each other. Throughout the paper, $\hat{\mathbf{a}}$ always refers to the final answer of the full CoT, not the final answer generated after exiting a CoT early. Furthermore, when referring to $\hat{\mathbf{a}}$ with respect to its position in a CoT, we always mean the *earliest logical arrival* of $\hat{\mathbf{a}}$ unless stated otherwise explicitly. By the earliest logical arrival of $\hat{\mathbf{a}}$, we are referring to the sequence of logical steps in the CoT that yields the final answer $\hat{\mathbf{a}}$ for the first time. For any early-exit strategy, a key metric to gauge its performance is the per-sample compression rate (CR): $\frac{M_{\text{early}}}{M}$, where $M_{\text{early}} \in [M]$ is the token index of early exit in \mathbf{r} . Accuracy (Acc) measures the proportion of problems where the correct answer is produced.

2.2. Hindsight-optimality

We now formally define our novel notion of hindsight-optimality. Given an input prompt $\mathbf{x} \in \mathcal{X}^L$ of length L over a vocabulary \mathcal{X} , an LRM LRM, which generates the corresponding CoT $\mathbf{r} \in \mathcal{X}^M$ and the solution $\mathbf{s} \in \mathcal{X}^N$ with the answer $\hat{\mathbf{a}} \in \mathcal{X}$, the hindsight-optimal reasoning length (HORL) is defined as the minimum of all indices $i \in [M]$ such that upon truncating the CoT at position i , i.e. $\mathbf{r}_{\leq i}$, LRM still produces the same final answer $\hat{\mathbf{a}}$. Mathematically,

$$\begin{aligned} \text{HORL}(\mathbf{x}, \mathbf{r}, \mathbf{s}, \hat{\mathbf{a}}; \text{LRM}) \\ \triangleq \min \{i \in [M] : \mathbf{s}' = \text{LRM}(\mathbf{x}, \mathbf{r}_{\leq i}) \text{ yields the answer } \hat{\mathbf{a}}\}. \end{aligned} \quad (1)$$

Note that HORL is well-defined as the above set of indices is always non-empty; the index M corresponding to the full length CoT already yields $\hat{\mathbf{a}}$. Hence, by definition $\text{HORL} \leq M$.

2.3. Token-Confidence

Our analytical experiments require a measure of LRM’s confidence during the generation of a CoT. To this end, we use the Token-Confidence metric, that gauges the uncertainty of a chosen token. Mathematically, for every $i \in [M]$, the corresponding Token-Confidence C_i is defined as

$$C_i \triangleq -\frac{1}{K} \sum_{k \in \mathcal{T}_K(i)} \log \mathbb{P}_{\text{LRM}}(r_i = k \mid \mathbf{x}, \mathbf{r}_{<i}), \quad (2)$$

where $\mathbb{P}_{\text{LRM}}(r_i = \cdot \mid \mathbf{x}, \mathbf{r}_{<i})$ is the LRM prediction probability at position i and $\mathcal{T}_K(i) \triangleq \text{Top-}K[\mathbb{P}_{\text{LRM}}(r_i = \cdot \mid \mathbf{x}, \mathbf{r}_{<i})]$ is the set of vocabulary tokens corresponding to the Top- K probabilities. In other words, Token-Confidence is the average (negative) log-probability across the Top- K probabilities (we set

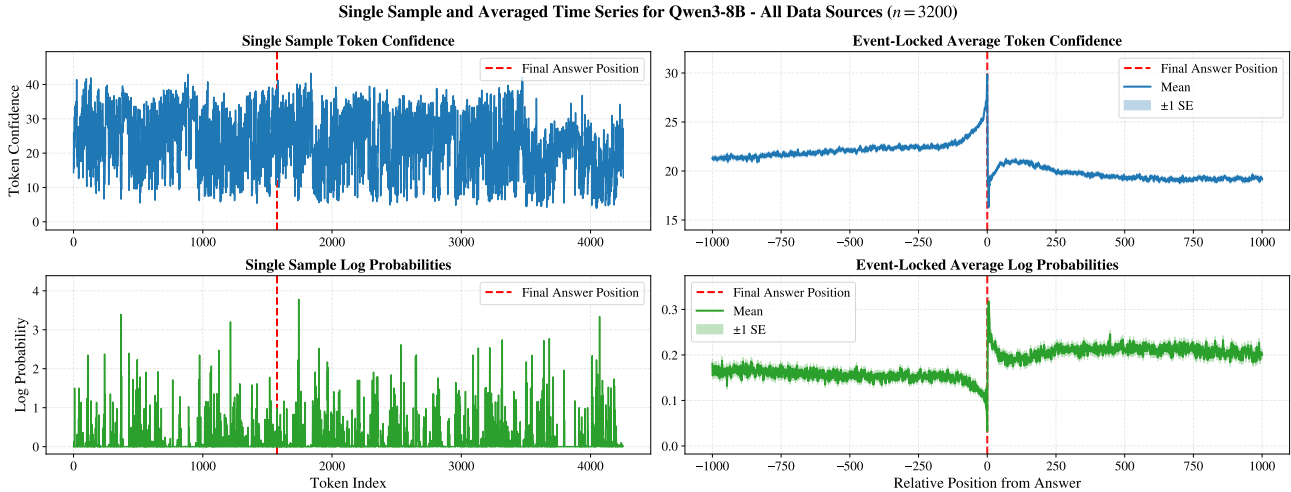


Figure 2. Event-Locked Averaging of Token-Confidence. Event-locked averaging shows a consistent agreement on spiking behavior at the answer position in each CoT, but disagrees elsewhere. On the other hand, this phenomenon is not readily observable in the single-sample case. Figures on the **left** show the Token-Confidence (Fu et al., 2025b) and log-probability trajectories throughout reasoning for a single, randomly selected sample; figures on the **right** show the effect of *event-locked averaging* on the position of the first arrival of the final answer across all CoTs. The 3200 CoTs used are a random subset of our training set, which combines AIME (1983–2024), MATH, OpenCoder-SFT, and OpenScience. Figs. 10 to 13 in App. B show similar trends for each dataset separately. Note that the Standard Error shown here as a shaded region is not readily noticeable but is more apparent with further zooming in.

$K = 20$ in our experiments). The higher it is, the more confident the model is in its predictions.

This measure is based on the Self-Certainty metric (Kang et al., 2025b), computed as the KL-divergence between the uniform distribution and the token distribution, and is based on the following idea: the higher the confidence of the model, the further its predictions should be from the uniform distribution. We also note that, while Token-level log-probabilities are commonly used as a proxy for confidence, we prefer the Token-Confidence measure (Fu et al., 2025b) here, as it is principled and produces less noise. Both are used, and the same conclusions can be drawn using either.

3. Motivation

Shortly after the breakthrough of LRMs, it was observed that they exhibit an overthinking phenomenon where, despite arriving at the correct answer, they continue to consider alternative solution paths, possibly leading to other incorrect answers (Chen et al., 2025; Luo et al., 2025). While LRMs achieve greatly improved performance over their non-reasoning counterparts, they do so at a much higher inference-time cost: up to thousands of additional tokens are generated to form the CoT before arriving at the final solution (Guo et al., 2025). Many follow-up works have observed the same overthinking phenomenon and developed methods to mitigate wasteful token expenditure (Zhang et al., 2025b; Liu & Wang, 2025; Wu et al., 2025a; Zhang et al., 2025a).

Towards designing an optimal early-exit strategy to stymie

overthinking, we build upon the following key observation: once an LRM generates a CoT r and a final solution s , we can observe the final answer \hat{a} . Then, *in hindsight*, we can determine precisely where the LRM should have exited the CoT to avoid wasting tokens, i.e. HORL, and instead generate the final solution. To this end, we first only need to check for \hat{a} , not a , in r , since the LRM may never even have generated the correct (ground-truth) answer and thus may not exist in r . Second, by choosing to terminate reasoning after the arrival of \hat{a} in r , all steps that are useful to arriving at \hat{a} are kept, and anything after is skipped as it is redundant.

While the above procedure requires the explicit knowledge of \hat{a} to check for its arrival, *are there meaningful markers to implicitly detect its arrival?*

Detecting the Answer Early. To this end, we ran experiments on AIME (1983–2024), MATH, OpenCoder-SFT, and OpenScience datasets to analyze trends in the Token-Confidence metric during CoT reasoning, illustrated in Figs. 2 and 3. In particular, Fig. 2 reveals a striking phenomenon: the arrival of \hat{a} is marked by a sharp transition in the Token-Confidence metric for event-locked averaged plots as opposed to single CoT plots. Here the event-locked average is formed by aligning the position of the first \hat{a} occurrence in each CoT’s signal to 0, and then taking the average across many CoTs. The CoTs are sampled from the above combined datasets, covering problems in math, science, and coding, showing that this behavior is consistent across different data sources. Figs. 10 to 13 in App. B show similar plots for each data source separately.

On the other hand, Fig. 3 analyzes the frequency of specific

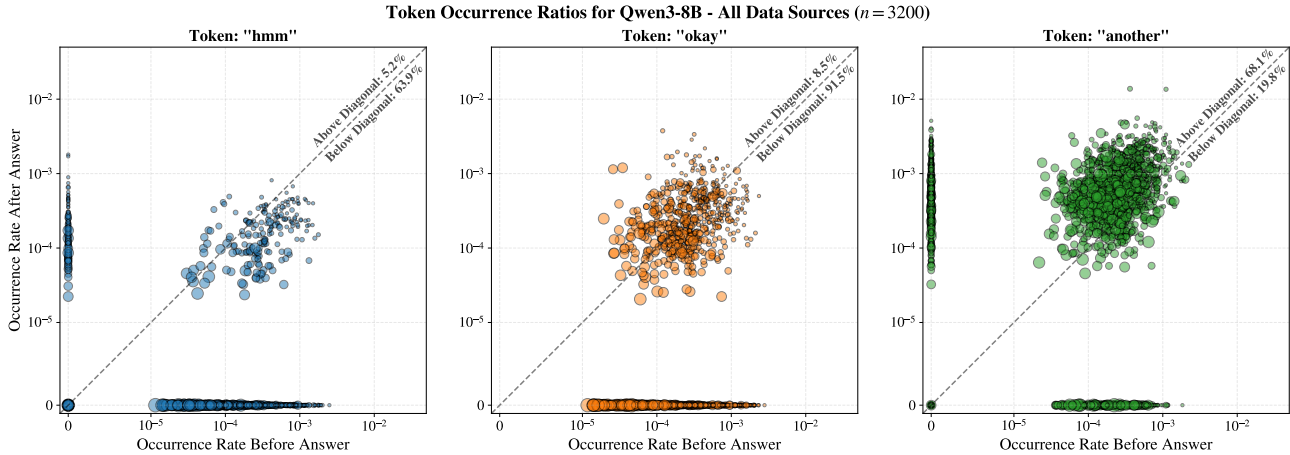


Figure 3. **Token Usage Frequency Shift.** “Thinking token” usage changes depending on whether the final answer has been generated in the CoT. Rates are computed by counting the raw number of occurrences of the token before and after the answer, and then normalizing each count by the respective number of tokens in the before and after bins. The arrival of the final answer is hinted at by changes in the rates for these tokens. The relative length of a CoT is captured by its dot size, where a longer CoT has a larger dot. App. B demonstrates similar results for other “thinking tokens” in Fig. 14 and for each data source in Figs. 15 to 18.

tokens before and after the first arrival of \hat{a} for three “thinking tokens,” of which `hmm` in the left plot, `okay` in the middle plot, and `another` in the right plot are shown. “Thinking tokens” are special tokens often associated with thinking, such as `wait`, `so`, `alternatively`, `hmm`, `therefore`, etc., that suggest ongoing reasoning patterns (Wang et al., 2025a; Qian et al., 2025; Ding et al., 2025). That is, their existence suggests a continuation of reasoning, which we aim to minimize, and we hypothesize that “thinking token” usage should change once \hat{a} has been generated. Indeed, all three plots in Fig. 3 show a bias in the token rates before and after the first occurrence of \hat{a} : `hmm` and `okay` occur more often before the answer, while `another` occurs more frequently after the answer. While not all “thinking tokens” show a clear bias before and after the answer is generated, this shift in the token-frequency distribution signals that \hat{a} has been generated (Fig. 14 in App. B illustrates similar trends for other “thinking tokens”). To clarify, each axis shows the frequency of the given token occurring before and after the answer, expressed as a rate computed as the raw count divided by the total number of tokens before and after the answer, respectively. The diameter of each point reflects the relative length of a CoT, where a smaller diameter corresponds to a shorter CoT and a larger diameter corresponds to a longer CoT.

Moving to Online Inference and Challenges. While these results strongly indicate the early arrival of \hat{a} , using them during online inference remains a challenge. In the case of Fig. 2, event-locked averaging requires multiple CoTs to be generated simultaneously, each with reasonable estimates of the position of the answer. Under those circumstances, the spiking behavior will emerge. But attaining a reasonable estimate of the answer position for a single CoT during inference is the original problem we

are tasked with. While applying the event-locked averaging signal to online inference is limited, it does indicate that an underlying trend can be extracted.

Similarly, each dot in Fig. 3 requires full knowledge of each r and its position of \hat{a} so that the rates can be calculated accordingly. Again, these results show a shift in the usage frequency of certain tokens before and after the first occurrence of \hat{a} , but translating the signal into an online inference algorithm remains challenging.

Our Approach. Under the hood of the LRM, there are clearly meaningful signals to indicate the earliest arrival of \hat{a} . However, as outlined above there are unique challenges in leveraging them in a hand-guided way to design an early-exit online inference algorithm. To address this, we approach this through the lens of *prediction*: i.e. predicting whether an LRM’s final answer \hat{a} has been generated or not. To this end, the core idea behind our method is to train a probe classifier on the hidden states of the final layer, thereby utilizing as many of the LRM’s underlying signals as possible. Prior work has examined hidden states to assess whether LRMs know when their intermediate CoT answers are correct (Zhang et al., 2025a), a finding primarily aimed at understanding model internals rather than designing practical early-exit methods at inference. Our work adopts a fundamentally different, deployable approach by probing for the *final answer* \hat{a} , a signal that is fully self-contained within the LRM’s reasoning process and requires no ground-truth labels at inference time, thereby enabling a principled early-exit strategy.

To train the probe classifier, we process inputs at the token level, offering much finer-grained predictions than prior work. That is, our dataset is curated for a token classification task. To the best of our knowledge, all

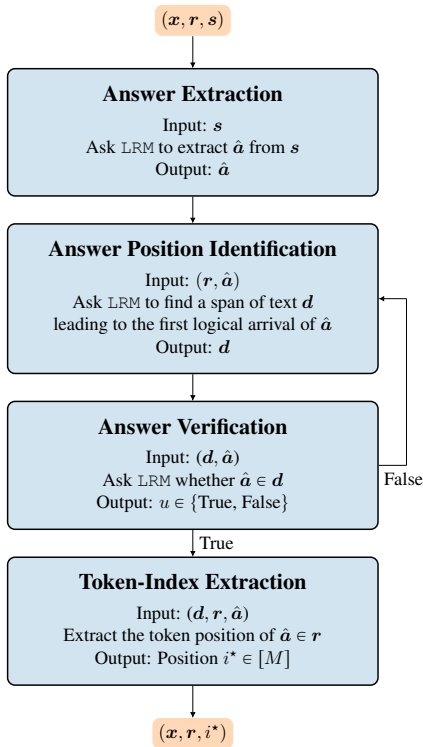


Figure 4. **Training-Dataset Curation Process.** We use an LRM to (1) extract final answer \hat{a} from final solution s , (2) identify the earliest position of \hat{a} in the CoT r , and (3) verify that the position was correct. If it was, then we can extract the exact position of \hat{a} from the CoT at the final token-index extraction step; otherwise, we retry the identification step with feedback.

previous methods use much coarser granularity in their training dataset where they chunk each CoT r according to some heuristic, such as “thinking tokens” or paragraph delimiters such as $\backslash n \backslash n$. Then, at inference time, they exit once the predicted probability crosses a data-calibrated threshold (Liu & Wang, 2025; Wu et al., 2025a; Zhang et al., 2025a). In contrast, our approach offers two-fold advantages at inference-time: (1) a probe classifier trained with our dataset has the ability to exit immediately after \hat{a} is generated, and (2) while our approach is amenable to using a data-calibrated threshold, it is not necessary. The main drawback of data-calibrated thresholding is that it requires additional samples from the evaluation data distribution, and the resulting threshold is therefore specific to that distribution and may not transfer well to other distributions.

However, obtaining the \hat{a} positions to create our HORN-dataset in a scalable way is challenging and highly non-trivial, which we precisely address in the next section.

4. TERMINATOR: Methodology

Given a full CoT and the corresponding final solution from an LRM, the earliest logical arrival to the LRM’s final answer can be detected in the CoT. However, reliable de-

tection for tens of thousands of CoTs is a unique challenge, which we address through our pipeline in Sec. 4.1. We then present our method for training TERMINATOR, which is a probe classifier, in Sec. 4.2.

4.1. Early Answer Extraction, Identification, and Verification

Our early answer extraction, identification, and verification pipeline (Fig. 4) is a critical component of our data curation process; at its core is an LRM that (1) extracts the final answer \hat{a} from final solution s (answer extraction), (2) identifies the earliest logical arrival to \hat{a} in r (answer identification), (3) verifies that the extraction step was successful (answer verification). And finally (4) we extract the exact position of \hat{a} from the CoT (token-index extraction).

Rationale. Extracting the position of \hat{a} is not trivial. Human inspection and annotation of CoTs is one route, but it is expensive and not scalable. Our early attempts at answer extraction, identification, and verification relied solely on fuzzy pattern matching, leading to many false positives despite accommodating as many edge cases as possible. The primary challenge is that identifying the answer position within a CoT is a semantic search problem that cannot be reliably solved with fuzzy or regex pattern matching, which we illustrate by three failure modes:

1. **Numerical answers.** A numerical value may appear frequently throughout the CoT in intermediate calculations, problem restatements, or discarded solution attempts, making it impossible to distinguish these occurrences from the true final answer by pattern alone. For example, if the final answer is $x = 42$, the value 42 may appear dozens of times in prior reasoning steps.
2. **Mathematical expressions.** The same mathematical object can be represented in many syntactically distinct forms. For instance, x^2 , $x**2$, $\text{pow}(x, 2)$, and $x \cdot x$ are semantically equivalent but would not be matched by any single pattern. Differences in $\text{L}^{\text{T}}\text{E}^{\text{X}}$ formatting, Unicode symbols, and whitespace further compound this.
3. **Python functions.** A Python function may not appear as a contiguous block anywhere in the CoT; instead, it may be generated line by line, interspersed with commentary. The final reconstructed answer, therefore, does not exist verbatim in the text, making positional matching fundamentally ill-posed.

Using an LRM for all three steps confirmed that the earliest answer positions can be reliably extracted.

Our Extract-Identify-Verify Pipeline. First, the final answer \hat{a} needs to be extracted from s . The answer itself is

clearly marked, e.g. using `\boxed{ }` to mark the answer, so \hat{a} is easily extracted by the LRM. Then, the LRM’s task in the answer identification step is not just to locate the answer, but to return a span of text d that leads up to and includes \hat{a} . This strategy ensures that d is a unique substring of r that can be used later to find the exact token position of the earliest occurrence of \hat{a} . Once d is obtained, the LRM is tasked with verifying that d does indeed contain \hat{a} .

The answer identification and answer verification steps form a two-step procedure with a feedback loop: if \hat{a} is not found in d , the LRM returns to the answer identification step with textual feedback containing all previously identified spans that did not contain \hat{a} . This approach allows the LRM to try again while reducing the risk that it will choose the same span in the new attempt. If the model fails to identify a span that contains \hat{a} within a max retry limit, that CoT will not be added to the training dataset. If the verification step is successful, d is located within r , and the earliest answer token position i^* is retrieved. Algorithm 1 in Sec. A.1 shows the pseudocode for our early answer extraction, identification, and verification method. Together, these steps help create our HORL-dataset in a scalable way, on which we train our probe classifier.

4.2. TERMINATOR: Binary Probing Classifier

Our approach entails training a small classification model θ on the LRM’s final-layer hidden states h_i and making a binary prediction b_i at each CoT position $i \in [M]$ (Fig. 1). More specifically, our model reuses the same transformer block from the LRM and adds a prediction head. The weights of the transformer block are copied from the final block of the LRM, which we found performs slightly better than random initialization, and the prediction head is randomly initialized. During training, the task is to predict whether the first occurrence of the final answer has been generated (label 1) or not (label 0). Given the causality of the transformer block, every prediction depends on the history of the CoT up to that point, but the predictions themselves are made independently of each other. Due to the inherent class imbalance of this early-exiting prediction task, our model is trained with class-weighted binary cross-entropy loss, which for a single sample (x, r, s, i^*) is computed as:

$$L(\theta) = -\frac{1}{M} \sum_{i=1}^M \left[w_1 \cdot y_i \cdot \log p_i + w_0 \cdot (1 - y_i) \cdot \log(1 - p_i) \right], \quad (3)$$

where $y_i = \mathbb{1}(i < i^*) \in \{0, 1\}$ denotes the ground-truth label corresponding to answer arrival and $p_i = \mathbb{P}_\theta(b_i = 1 \mid x, r_{\leq i})$ is the predicted probability for each $i \in [M]$, with M being the CoT length, and w_0 and w_1 the class weights. These weights are automatically computed from the training dataset using inverse frequency weighting as shown in Eq. (4), where n_0 and n_1 are the total

number of 0 and 1 labels in the training dataset, respectively:

$$w_0 = \frac{n_0 + n_1}{2n_0}, \quad w_1 = \frac{n_0 + n_1}{2n_1}. \quad (4)$$

Here we note that TERMINATOR is inspired by the findings of optimal-length reasoning literature; we seek to train a model on hindsight-optimal CoTs to encourage TERMINATOR to early-exit as soon as the final answer is generated. Unlike other methods, TERMINATOR is free of data-calibrated thresholding and is trained on several data sources (math, coding, and STEM problems) simultaneously.

5. Experiments

5.1. Implementation Details

Models. We train and evaluate our method on LRMs from two different model families: Qwen3-8B and Qwen3-14B (Yang et al., 2025a), and Ministral-3-8B-Reasoning-2512 and Ministral-3-8B-Reasoning-2512 (Liu et al., 2026). We use Qwen3-30B-A3B-Thinking-2507 for our answer extraction, identification, and verification pipeline. Our trained models consist of a single transformer layer initialized from the final layer of the LRM and a binary prediction head. We compare TERMINATOR against (1) prompt-based approaches, including Vanilla, NoThinking (Ma et al., 2025a), DEER (Yang et al., 2025b), and Dynasor (Fu et al., 2025a), and (2) a probe-based approach, Thought Calibration (Wu et al., 2025a). Vanilla is a direct evaluation of the LRM without any intervention. NoThinking prompts the model to skip the reasoning phase and generate the final solution s directly. DEER splits the reasoning into chunks, checks the average token probability after every chunk, and exits if it exceeds a threshold. Dynasor periodically prompts the model to produce intermediate answers at fixed token intervals and triggers early exit when 8 consecutive answers are consistent. Thought calibration trains linear probes on the hidden representations of reasoning steps to automatically decide when to stop generation. We retrain these probes for our 4 models using their *Supervised* method. For further details of the baselines’ implementations, we refer to Sec. A.3.

Datasets. We form a training data mix with AIME (1983–2024) (Art of Problem Solving), MATH (Lightman et al., 2024), OpenCoder-SFT (Huang et al., 2024), and OpenScience (NVIDIA, 2025). We form our training datasets by sampling three CoTs from each of these datasets, identifying the answer positions (see Sec. 4.1), and assigning the corresponding training labels. We evaluate our method and all baselines on AIME 2025 (Art of Problem Solving), MATH-500 (Lightman et al., 2024), HumanEval (Chen et al., 2021), and GPQA (Rein et al., 2024). Additional details on our training datasets are available in Appendix A.2.

Training and Inference. During training, we optimize for high performance on a holdout validation set for

TERMINATOR : Learning Optimal Exit Points for Early Stopping in Chain-of-Thought Reasoning

Table 1. Performance of TERMINATOR and Baselines. \uparrow Indicates that higher values are better, while \downarrow indicates that lower values are better. CR is the compression rate, reported here as the mean per-sample compression rate. Tok is the mean number of tokens per sample. **Bold** and Underlined values highlight the best and second-best performing early exit methods, respectively. TERMINATOR demonstrates superior accuracy-efficiency trade-offs (best or second-best performance across 28 out of 32 metrics). Fig. 9 in App. B shows the results of this table on the Pareto frontier.

| Method | Math | | | | | | Coding | | | Science | | | Overall | |
|---------------------------------------|----------------|------------------|-----------------|----------------|------------------|-----------------|----------------|------------------|-----------------|----------------|------------------|-----------------|----------------|-----------------|
| | MATH-500 | | | AIME25 | | | HumanEval | | | GPQA | | | Acc \uparrow | CR \downarrow |
| | Acc \uparrow | Tok \downarrow | CR \downarrow | Acc \uparrow | Tok \downarrow | CR \downarrow | Acc \uparrow | Tok \downarrow | CR \downarrow | Acc \uparrow | Tok \downarrow | CR \downarrow | | |
| Qwen3-8B | | | | | | | | | | | | | | |
| Vanilla | 91.1% | 5,037 | 100% | 74.4% | 14,499 | 100% | 86.4% | 3,792 | 100% | 57.6% | 8,594 | 100% | 77.4% | 100% |
| NoThinking | 80.7% | 809 | 16.1% | 22.0% | 2,355 | 18.6% | 78.5% | 353 | 11.8% | 30.7% | 1,204 | 15.8% | 53.0% | 15.6% |
| DEER | 79.9% | 2,602 | 52.0% | 21.4% | 10,349 | <u>67.8%</u> | 77.4% | 3,275 | 83.6% | 50.5% | 8,553 | 99.6% | 57.3% | 75.8% |
| Thought-Calib | <u>90.1%</u> | 4,372 | 93.9% | <u>65.8%</u> | 11,014 | 81.5% | 71.8% | 3,267 | 92.9% | 52.6% | 6,240 | <u>78.9%</u> | <u>70.1%</u> | 86.8% |
| Dynasor | 78.3% | 1,850 | 41.0% | 48.0% | 7,479 | 48.8% | <u>79.3%</u> | 2,883 | <u>78.4%</u> | 43.2% | 2,455 | 28.4% | 62.2% | 49.2% |
| TERMINATOR | 90.7% | 2,425 | <u>45.1%</u> | 69.4% | 10,970 | 70.7% | 82.9% | 2,716 | 69.9% | <u>52.1%</u> | 7,543 | 85.7% | 72.6% | <u>67.8%</u> |
| Qwen3-14B | | | | | | | | | | | | | | |
| Vanilla | 92.0% | 4,598 | 100% | 79.9% | 14,255 | 100% | 76.0% | 3,296 | 100% | 59.9% | 7,628 | 100% | 77.0% | 100% |
| NoThinking | 84.1% | 786 | 17.5% | 26.3% | 2,472 | 19.9% | 78.3% | 317 | 12.2% | 32.1% | 1,265 | 18.8% | 55.2% | 17.1% |
| DEER | 80.9% | 2,501 | 56.2% | 27.6% | 10,497 | <u>71.0%</u> | 80.7% | 2,961 | 87.3% | 49.0% | 7,451 | 97.4% | 59.6% | 78.0% |
| Thought-Calib | <u>89.8%</u> | 3,778 | 92.0% | <u>63.3%</u> | 9,429 | 71.3% | 74.8% | 2,582 | 87.1% | 54.6% | 5,757 | <u>81.9%</u> | <u>70.6%</u> | 83.1% |
| Dynasor | 79.6% | 1,702 | 42.4% | 61.8% | 7,937 | 52.8% | 83.9% | 2,611 | <u>82.2%</u> | 45.6% | 2,101 | 29.1% | 67.7% | 51.6% |
| TERMINATOR | 90.7% | 2,261 | 46.8% | 74.2% | 10,787 | <u>71.0%</u> | <u>83.3%</u> | 2,358 | 70.9% | <u>53.9%</u> | 6,798 | 87.1% | 78.0% | <u>65.0%</u> |
| Ministral-3-8B-Reasoning-2512 | | | | | | | | | | | | | | |
| Vanilla | 93.5% | 6,212 | 100% | 92.6% | 22,124 | 100% | 92.1% | 4,367 | 100% | 62.3% | 11,765 | 100% | 85.1% | 100% |
| NoThinking | 83.2% | 1,908 | 28.1% | 43.6% | 7,711 | 36.5% | 70.5% | 727 | 16.4% | 39.7% | 2,106 | 16.0% | 59.3% | 14.6% |
| DEER | 71.0% | 3,791 | 60.3% | 67.1% | 17,481 | 77.0% | 75.8% | 3,606 | <u>84.0%</u> | 61.1% | 11,312 | 94.1% | 68.8% | 78.9% |
| Thought-Calib | 87.7% | 5,695 | 87.8% | <u>83.7%</u> | 20,358 | 91.2% | 47.2% | 3,536 | 87.2% | 47.3% | 7,406 | 71.8% | 66.5% | 84.5% |
| Dynasor | <u>88.1%</u> | 2,967 | <u>56.8%</u> | 87.6% | 15,407 | 66.3% | 92.1% | 3,931 | 88.6% | 51.8% | 9,766 | 83.7% | 79.9% | <u>73.9%</u> |
| TERMINATOR | 89.1% | 2,863 | 47.8% | 57.4% | 15,239 | <u>67.1%</u> | <u>89.0%</u> | 2,960 | 66.6% | <u>58.2%</u> | 9,588 | <u>77.4%</u> | <u>73.4%</u> | 64.7% |
| Ministral-3-14B-Reasoning-2512 | | | | | | | | | | | | | | |
| Vanilla | 93.0% | 6,385 | 100% | 88.1% | 23,694 | 100% | 89.6% | 3,918 | 100% | 62.7% | 9,539 | 100% | 83.4% | 100% |
| NoThinking | 79.1% | 535 | 11.7% | 20.5% | 2,413 | 13.8% | 80.0% | 528 | 14.1% | 41.0% | 570 | 6.6% | 55.2% | 13.7% |
| DEER | 69.8% | 4,279 | 74.6% | 55.9% | 20,049 | 84.9% | 19.3% | 1,684 | 46.5% | <u>58.5%</u> | 9,185 | 95.0% | 50.9% | 75.3% |
| Thought-Calib | <u>87.3%</u> | 5,860 | 95.9% | 59.4% | 17,763 | 79.8% | 27.6% | 3,465 | 96.3% | 49.5% | 6,028 | 73.8% | 56.0% | 86.5% |
| Dynasor | 86.3% | 3,240 | <u>55.5%</u> | 83.2% | 17,920 | <u>70.6%</u> | 86.8% | 3,538 | 88.9% | 51.3% | 7,917 | 85.2% | 76.9% | <u>75.1%</u> |
| TERMINATOR | 90.2% | 2,946 | 43.9% | <u>65.8%</u> | 15,898 | 68.7% | 89.6% | 2,903 | <u>71.0%</u> | 60.6% | 7,727 | <u>76.5%</u> | <u>76.5%</u> | 65.0% |

our prediction task; we choose our model based solely on how well it performs on the binary predictive task, without peeking at the evaluation dataset performance. Our validation metric of choice is the Macro-F1 score.

We use vLLM (Kwon et al., 2023) with asynchronous requests to sample CoTs when curating our training datasets. During inference with our trained model, a sliding window of the 10 most recent predictions is used, and the `</think>` token is injected when more than 50% of the labels are 1 (majority voting). We set the threshold of predicting 1 to 0.7.

5.2. TERMINATOR: Main Results

Table 1 shows the performance of TERMINATOR and relevant baselines with respect to the Compression Rate (lower is better) and Accuracy (higher is better). To ensure a fair comparison, all methods are evaluated using the same CoTs that are used in the vanilla baseline, except

the NoThinking baseline, for which no CoT is generated. TERMINATOR achieves best or second best performance on 28 out of 32 metrics, and achieves a better overall compression-performance trade-off over prior methods on the Pareto frontier as shown in Fig. 9. Notably, while methods such as *Dynasor* achieve aggressive token reduction, they do so at the cost of significant accuracy degradation. TERMINATOR consistently occupies a favorable position on the accuracy-efficiency Pareto frontier across all four evaluated LRMs, demonstrating that its advantages are robust to model architecture and scale.

5.3. Ablation studies

We run ablation studies of TERMINATOR with respect to (1) out-of-distribution (OOD) performance, (2) its performance against the truncated early-exit baseline, and (3) latency and throughput over the vanilla baseline. Our results in this section will be reported mostly on Qwen3-8B alone, with re-



Figure 5. OOD Performance of TERMINATOR. The best trade-off between accuracy and compression rate is achieved when the evaluation set is in-distribution with the training dataset. Here the out-of-distribution performance of TERMINATOR with respect to the compression rate (left) and the accuracy (right) for Qwen3-8B is shown. Training datasets are listed along the row axis, and the evaluation sets are listed across the column axis. For example, training TERMINATOR on MATH and evaluating on HumanEval yields a compression rate of 67% and an accuracy of 83%. Every training dataset has an in-domain evaluation dataset, i.e. MATH \rightarrow MATH-500, AIME 1983–2024 \rightarrow AIME25, OpenCoder-SFT \rightarrow HumanEval, and OpenScience \rightarrow GPQA.

sults on Qwen3-14B, Ministral-3-8B, and Ministral-3-14B reported in Table 1 and Fig. 9. Beyond what is presented here, additional supplemental results are provided in App. B.

Out-of-Distribution Evaluation. To better understand the out-of-distribution performance of TERMINATOR, we separately train on each of the four tasks that make up our training dataset, and evaluate each resulting model on the test datasets. Fig. 5 shows heatmaps for the compression rate and the accuracy, where the row and column axes correspond to the training dataset and the testing dataset, respectively, and the value indicates the performance on the testing dataset. These results yield two key insights: (i) the best compression rate is achieved when the test dataset is in-distribution with the training dataset (i.e. along the diagonal). However, (ii) the best accuracy is not always on the diagonal; this is especially true for AIME25 evaluation, where training on AIME (1983–2024) yields the *lowest* accuracy. This makes sense when considering the compression rates for AIME25, as the better compression rates correspond to the lowest accuracy. This behavior does not happen with the other datasets, suggesting two things: (1) TERMINATOR tends to be overconfident on challenging tasks like AIME25 and is exiting too early, and (2) TERMINATOR is less confident when training on simpler tasks, thereby prolonging reasoning (worse compression rate) and increasing the accuracy. Training on OpenCoder-SFT shows behavior similar to item (2), yielding high (often the best) accuracy scores across all test sets but also the worst compression rates. This suggests that training to early-exit for coding tasks is not as useful for determining the early-exit position for the other tasks.

Hindsight-Optimal CoTs. Since TERMINATOR is trained on hindsight-optimal reasoning length (HORL) CoTs, it is natural to ask where TERMINATOR lies on the

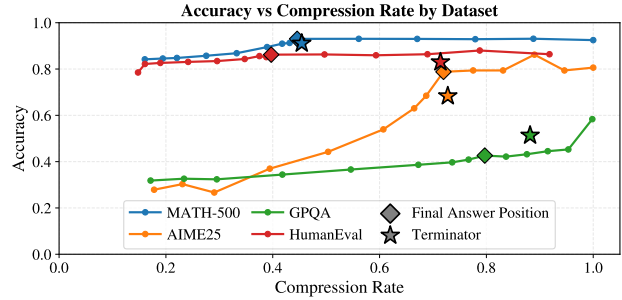


Figure 6. Effects of Early CoT Termination. Test set CoTs are evaluated after truncating them at various points via `</think>` and asking the LRM for a final solution and answer. Diamond-shaped points show the hindsight-optimal reasoning length, and TERMINATOR falls close to optimality for three out of the four datasets.

accuracy-compression frontier relative to the ground-truth HORL. Fig. 6 shows the accuracy with respect to CoT progress. Each dot on the curves represents the average accuracy when each CoT was truncated early, and the LRM was forced to give a final solution and final answer. We vary the truncation positions to cover the entire range of compression rates. The diamond-shaped dots represent the position of the first occurrence of \hat{a} , and therefore represent the points where hindsight-optimal reasoning is achieved. As expected, the accuracy remains relatively constant after this point, suggesting that additional reasoning beyond \hat{a} does not yield significant accuracy gains, if any. We plot TERMINATOR alongside these curves to show how close it is to the hindsight-optimal CoT length and performance. Notably, TERMINATOR is close to hindsight-optimality for MATH-500, AIME25, and HumanEval, but is quite far from the hindsight-optimal compression rate for GPQA. This suggests that GPQA is a challenging dataset for TERMINATOR to generalize to, but it might be improved with a more rigorous data curation process for GPQA-style questions.

Latency Analysis. We develop a vLLM-compatible implementation of TERMINATOR, benchmark the latency and throughput, and compare with running the vanilla LRM in vLLM. The results are presented in Table 2. Both methods are evaluated on the same subset of MATH-500 questions with a batch size of 1, disabled prefix caching, and on a single GH200. TERMINATOR halves the average latency over the vanilla LRM, but does incur a small overhead of 10.8% for Qwen3-8B and 7.5% for Qwen3-14B. However, as the base LRM size increases, TERMINATOR incurs a proportionally smaller overhead since its architecture (a single transformer layer and an FFN) remains fixed.

5.4. Early-Exit Signal Analysis

The results shown in Figs. 2 and 3 motivate our approach by confirming that the first arrival of \hat{a} is (1) marked by spiking behavior in the Token-Confidence, which is

Token Confidence Comparison: Ground Truth vs. Terminator (Qwen3-8B) - All Test Samples (n = 1132)

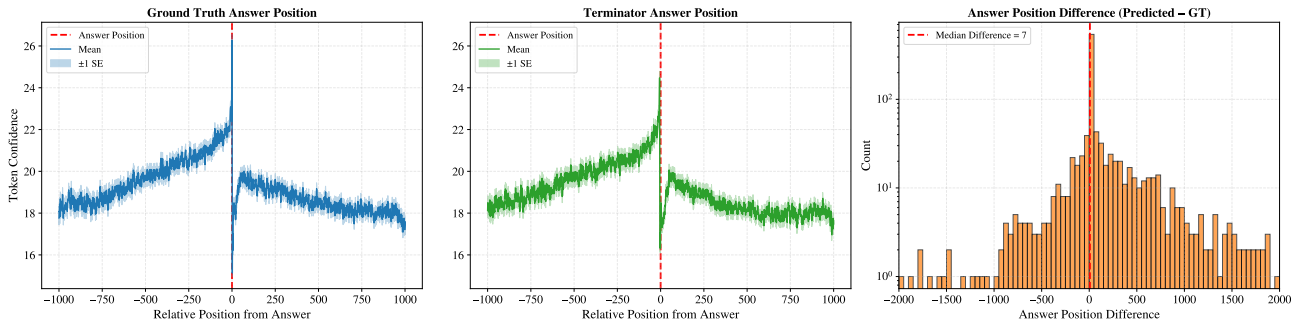


Figure 7. **TERMINATOR Recovers Event-Locked Average Spiking.** The exit positions predicted by TERMINATOR (center) recover the same spiking behavior in the event-locked averaged Token-Confidence as the ground-truth answer positions (left). The histogram of differences between the exit positions (right) shows that TERMINATOR’s predicted exit positions are close to the ground-truth. Note that the y-axis on the histogram is log-scaled.

Table 2. **Latency Analysis.** Latency and throughput benchmarks on MATH-500 problems (batch size 1) for Qwen3-based vanilla and TERMINATOR models. TERMINATOR reduces latency costs by a factor of over 2×, but does incur a slight throughput overhead. Values are reported as the mean ± 95% CI.

| Method | Latency (s) | Throughput (tok/s) |
|------------------|---------------|--------------------|
| Qwen3-8B | | |
| Vanilla | 32.68 ± 9.59 | 151.5 ± 4.4 |
| Terminator | 14.10 ± 6.27 | 135.2 ± 2.0 |
| Qwen3-14B | | |
| Vanilla | 43.38 ± 13.98 | 98.0 ± 2.0 |
| Terminator | 18.76 ± 6.52 | 90.6 ± 0.8 |

most easily seen in the event-locked average case, and (2) by a shift in the “thinking token” usage distribution. Focusing on the averaged plots in Fig. 2, we observe that the confidence of the LRM grows up to the point when \hat{a} is first generated, where the confidence finally peaks. The confidence immediately drops after \hat{a} is generated, which is intuitive given that the LRM immediately begins to doubt itself, often producing “thinking tokens” like wait or but, signaling uncertainty about the answer that was just generated. The LRM’s confidence improves slightly as it continues to rethink the problem.

TERMINATOR Recovers Early-Exit Signals. Using TERMINATOR’s predicted exit positions, the same event-locked averaging (Fig. 2) and “thinking token” frequency (Fig. 3) phenomena are recovered. Fig. 7 mirrors Fig. 2, but uses all samples from the test datasets instead of 3,200 randomly selected samples from our training dataset (gathering TERMINATOR’s predictions on the 3,200 samples requires additional compute; the test dataset predictions are readily available). The leftmost panel shows the event-locked average Token-Confidence based on the ground-truth answer positions, while the center panel shows the event-locked average Token-Confidence using the answer positions predicted by TERMINATOR. The rightmost panel shows the

histogram of differences between TERMINATOR’s predicted exit positions and the ground-truth positions; these differences are concentrated around zero, with a median difference of 7, which helps explain why TERMINATOR recovers most of the same signal.

Similarly, Fig. 8 is analogous to Fig. 3, but superimposes the resulting scatter plots when the ground-truth answer positions are used and when TERMINATOR’s answer positions are used. Inset axes show that the above-diagonal percentages are nearly the same between these two, demonstrating that the “thinking token” occurrence rates before and after TERMINATOR’s predicted answer positions reveal before/after token usage biases.

The results of Figs. 7 and 8 together show that training TERMINATOR on the LRM’s hidden states is enough for TERMINATOR to independently recover the same early-exit signals discovered earlier.

Event-Related Potentials for LRMs. We liken the averaged result in Fig. 2 to the field of *event-related potential* (ERP) research. An ERP is a measurable brain response elicited by a sensory, cognitive, or motor event, captured by electroencephalogram (EEG) recordings (Luck, 2014). However, EEG recordings are often noisy, so ERPs are estimated using time-locked statistical estimators (e.g. averaging) across multiple EEG trials. While we do not claim that our findings will align exactly with ERP research, it is quite interesting that meaningful and observable signals can be extracted from LRMs using similar approaches, and we believe this warrants further exploration in future work.

Thinking Token Usage. Beyond providing motivation for our method, the results of Fig. 3 offer some interesting insights on the usage of “thinking tokens.” These plots show the strong usage bias that can occur with respect to the first occurrence of \hat{a} . For example, 63.9% and 91.5% of CoTs contain the tokens *hmm* and *okay* more often before \hat{a} than after it, respectively. Other tokens,

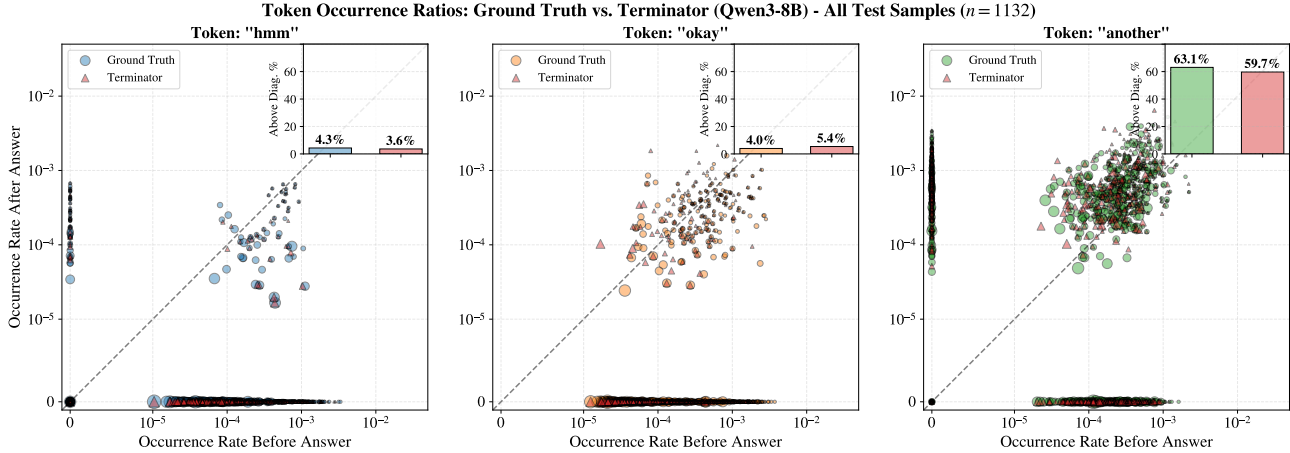


Figure 8. **TERMINATOR Token Usage Biases.** The exit positions predicted by TERMINATOR recover the same biases in the “thinking token” occurrence rates as the ground-truth answer positions. The inset axes on each panel show the percentage of dots that lie above the diagonal when the ground-truth and TERMINATOR answer positions are used.

like `another` are more frequently used after. Moreover, Figs. 14 to 18 in App. B show that the occurrence rates can differ drastically between data sources. For example, the token `alternatively` has an above-diagonal rate of 80.4% for MATH, but only 19.2% for OpenCoder-SFT.

Fig. 3 also shows the length of each CoT by its dot size; it appears that there is some correlation between the dot size and the occurrence rates. We show plots of the before and after occurrence rates for these three tokens in Fig. 19. Notably, shorter CoTs do in fact correlate with higher token occurrences for these three “thinking tokens.”

6. Related Work

Prompt Compression. This line of work is concerned with compressing the input prompt (or context) before passing it to an LLM. Some methods use *soft-prompts* (Mu et al., 2023; Chevalier et al., 2023; Ge et al., 2024; Qin et al., 2024) to compress tokenized inputs into a sequence of embeddings. These embeddings serve as the LLM’s input, allowing richer expressivity, but they are not amenable to black-box LLMs and are difficult to analyze theoretically. Other methods use *hard-prompts* (Jung & Kim, 2024; Jiang et al., 2024; Pan et al., 2024; Nagle et al., 2024), keeping the final compressed input prompt fixed to the same token vocabulary as the LLM.

Efficient Reasoning. Analogously to soft-prompt compression, *latent* or *continuous* reasoning is a technique where reasoning unfolds across latent output embeddings (or hidden states) rather than discrete tokens. Methods like Coconut (Hao et al., 2025), CCoT (Cheng & Durme, 2024), and Soft Thinking (Zhang et al., 2025d) feed the LLM’s output embeddings back into the input of the LLM during the reasoning stage, which significantly decreases the number of passes through the LLM before arriving at the final answer. LightThinker (Zhang et al., 2025c) uses

an idea similar to AutoCompressor (Chevalier et al., 2023), where each reasoning step is generated as discrete tokens first, compressed, and then the compressed summary of the reasoning thus far is fed back into the LLM to generate the next step. Other methods, like TokenSkip and C3oT (Xia et al., 2025; Kang et al., 2025a), are closer to hard-prompt compression, where a prompt compressor (or a summarization) model first compresses the CoTs into much shorter versions, and the LLM is retrained on these shorter CoTs. CoT-Valve (Ma et al., 2025b) extends this idea by introducing a parameter that adds explicit control over the reasoning length after fine-tuning. CALM (Schuster et al., 2022) also keeps its outputs in the token space, but saves compute by making layer-wise token-level early-exit decisions.

Early-Exit Reasoning. These methods seek to make reasoning more efficient by terminating the CoT early. All existing methods use a consistency-based approach, injecting the `</think>` token at various points to force the model to generate an answer or a useful signal. Some methods, like EAT (Wang et al., 2025b), DEER (Yang et al., 2025b), ES-CoT (Mao et al., 2025), and Dynasor (Fu et al., 2025a) are training-free; they track signals throughout the reasoning process and exit when a threshold is crossed. Other methods, like SpecExit (Yang et al., 2025c), Learn To Stop (Liu & Wang, 2025), Thought Calibration (Wu et al., 2025a), and FlashThink (Jiang et al., 2025) rely on training a separate probe classifier by using consistency as the main approach for gathering their training signals. By contrast, our work constructs a training signal to predict the immediate arrival of \hat{a} , thereby training on hindsight-optimal length CoTs. In addition, our work does not require threshold tuning on validation data, which is needed for Learn To Stop and Thought Calibration.

7. Conclusion

We present TERMINATOR, an early-exit method for LRM reasoning. Training TERMINATOR requires an optimal-length dataset of CoTs, which are obtainable through our robust answer extraction, identification, and verification pipeline. Furthermore, we provide novel analysis and insights into the behaviors of an LRM’s (1) Token-Confidence during reasoning (Fig. 2), and (2) shift in “thinking token” usage. While our training data curation pipeline works well, future work can explore making training more efficient as tens of thousands of CoTs are used to train TERMINATOR.

Acknowledgements

This work was partly supported by ARO Award W911NF2310062, ONR Award N000142412542, NSF 2443857 and the 6G@UT center within the Wireless Networking and Communications Group (WNCG) at the University of Texas at Austin. Our work used the Vista cluster at the Texas Advanced Computing Center (TACC) at The University of Texas at Austin. We thank TACC for providing the high-performance computing resources that supported this research.

References

- Art of Problem Solving. Aime problems and solutions. https://artofproblemsolving.com/wiki/index.php/AIME_Problems_and_Solutions. Accessed: 2026-01-07.
- Chen, M., Tworek, J., Jun, H., Yuan, Q., de Oliveira Pinto, H. P., Kaplan, J., Edwards, H., Burda, Y., Joseph, N., Brockman, G., Ray, A., Puri, R., Krueger, G., Petrov, M., Khlaaf, H., Sastry, G., Mishkin, P., Chan, B., Gray, S., Ryder, N., Pavlov, M., Power, A., Kaiser, L., Bavarian, M., Winter, C., Tillet, P., Such, F. P., Cummings, D., Plappert, M., Chantzis, F., Barnes, E., Herbert-Voss, A., Guss, W. H., Nichol, A., Paino, A., Tezak, N., Tang, J., Babuschkin, I., Balaji, S., Jain, S., Saunders, W., Hesse, C., Carr, A. N., Leike, J., Achiam, J., Misra, V., Morikawa, E., Radford, A., Knight, M., Brundage, M., Murati, M., Mayer, K., Welinder, P., McGrew, B., Amodei, D., McCandlish, S., Sutskever, I., and Zaremba, W. Evaluating large language models trained on code. *CoRR*, abs/2107.03374, 2021. URL <https://arxiv.org/abs/2107.03374>.
- Chen, X., Xu, J., Liang, T., He, Z., Pang, J., Yu, D., Song, L., Liu, Q., Zhou, M., Zhang, Z., Wang, R., Tu, Z., Mi, H., and Yu, D. Do NOT think that much for $2+3=?$ on the overthinking of long reasoning models. In *Forty-second International Conference on Machine Learning*, 2025. URL <https://openreview.net/forum?id=MSbU3L7V00>.
- Cheng, J. and Durme, B. V. Compressed chain of thought: Efficient reasoning through dense representations, 2024. URL <https://arxiv.org/abs/2412.13171>.
- Chevalier, A., Wettig, A., Ajith, A., and Chen, D. Adapting language models to compress contexts. In Bouamor, H., Pino, J., and Bali, K. (eds.), *Proceedings of the 2023 Conference on Empirical Methods in Natural Language Processing*, pp. 3829–3846, Singapore, December 2023. Association for Computational Linguistics. doi: 10.18653/v1/2023.emnlp-main.232. URL <https://aclanthology.org/2023.emnlp-main.232/>.
- Ding, B., Chen, Y., Wang, F., Ming, L., and Lin, T. Do thinking tokens help or trap? towards more efficient large reasoning model, 2025. URL <https://arxiv.org/abs/2506.23840>.
- Fu, Y., Chen, J., Zhu, S., Fu, Z., Dai, Z., Zhuang, Y., Ma, Y., Qiao, A., Rosing, T., Stoica, I., and Zhang, H. Efficiently scaling llm reasoning with certainindex, 2025a. URL <https://arxiv.org/abs/2412.20993>.
- Fu, Y., Wang, X., Tian, Y., and Zhao, J. Deep think with confidence, 2025b. URL <https://arxiv.org/abs/2508.15260>.
- Gao, J., Yan, S., Tan, Q., Yang, L., Xu, S., Fu, W., Mei, Z., Lyu, K., and Wu, Y. How far are we from optimal reasoning efficiency?, 2025. URL <https://arxiv.org/abs/2506.07104>.
- Ge, T., Jing, H., Wang, L., Wang, X., Chen, S.-Q., and Wei, F. In-context autoencoder for context compression in a large language model. In *The Twelfth International Conference on Learning Representations*, 2024. URL <https://openreview.net/forum?id=uREj4ZuGJE>.
- Guo, D., Yang, D., Zhang, H., Song, J., Wang, P., Zhu, Q., Xu, R., Zhang, R., Ma, S., Bi, X., Zhang, X., Yu, X., Wu, Y., Wu, Z. F., Gou, Z., Shao, Z., Li, Z., Gao, Z., Liu, A., Xue, B., Wang, B., Wu, B., Feng, B., Lu, C., Zhao, C., Deng, C., Ruan, C., Dai, D., Chen, D., Ji, D., Li, E., Lin, F., Dai, F., Luo, F., Hao, G., Chen, G., Li, G., Zhang, H., Xu, H., Ding, H., Gao, H., Qu, H., Li, H., Guo, J., Li, J., Chen, J., Yuan, J., Tu, J., Qiu, J., Li, J., Cai, J. L., Ni, J., Liang, J., Chen, J., Dong, K., Hu, K., You, K., Gao, K., Guan, K., Huang, K., Yu, K., Wang, L., Zhang, L., Zhao, L., Wang, L., Zhang, L., Xu, L., Xia, L., Zhang, M., Zhang, M., Tang, M., Zhou, M., Li, M., Wang, M., Li, M., Tian, N., Huang, P., Zhang, P., Wang, Q., Chen, Q., Du, Q., Ge, R., Zhang, R., Pan, R., Wang, R., Chen,

- R. J., Jin, R. L., Chen, R., Lu, S., Zhou, S., Chen, S., Ye, S., Wang, S., Yu, S., Zhou, S., Pan, S., Li, S. S., Zhou, S., Wu, S., Yun, T., Pei, T., Sun, T., Wang, T., Zeng, W., Liu, W., Liang, W., Gao, W., Yu, W., Zhang, W., Xiao, W. L., An, W., Liu, X., Wang, X., Chen, X., Nie, X., Cheng, X., Liu, X., Xie, X., Liu, X., Yang, X., Li, X., Su, X., Lin, X., Li, X. Q., Jin, X., Shen, X., Chen, X., Sun, X., Wang, X., Song, X., Zhou, X., Wang, X., Shan, X., Li, Y. K., Wang, Y. Q., Wei, Y. X., Zhang, Y., Xu, Y., Li, Y., Zhao, Y., Sun, Y., Wang, Y., Yu, Y., Zhang, Y., Shi, Y., Xiong, Y., He, Y., Piao, Y., Wang, Y., Tan, Y., Ma, Y., Liu, Y., Guo, Y., Ou, Y., Wang, Y., Gong, Y., Zou, Y., He, Y., Xiong, Y., Luo, Y., You, Y., Liu, Y., Zhou, Y., Zhu, Y. X., Huang, Y., Li, Y., Zheng, Y., Zhu, Y., Ma, Y., Tang, Y., Zha, Y., Yan, Y., Ren, Z. Z., Ren, Z., Sha, Z., Fu, Z., Xu, Z., Xie, Z., Zhang, Z., Hao, Z., Ma, Z., Yan, Z., Wu, Z., Gu, Z., Zhu, Z., Liu, Z., Li, Z., Xie, Z., Song, Z., Pan, Z., Huang, Z., Xu, Z., Zhang, Z., and Zhang, Z. Deepseek-r1 incentivizes reasoning in llms through reinforcement learning. *Nature*, 645(8081):633–638, September 2025. ISSN 1476-4687. doi: 10.1038/s41586-025-09422-z. URL <http://dx.doi.org/10.1038/s41586-025-09422-z>.
- Hao, S., Sukhbaatar, S., Su, D., Li, X., Hu, Z., Weston, J., and Tian, Y. Training large language models to reason in a continuous latent space, 2025. URL <https://arxiv.org/abs/2412.06769>.
- Huang, S., Cheng, T., Liu, J. K., Hao, J., Song, L., Xu, Y., Yang, J., Liu, J. H., Zhang, C., Chai, L., Yuan, R., Zhang, Z., Fu, J., Liu, Q., Zhang, G., Wang, Z., Qi, Y., Xu, Y., and Chu, W. Opencoder: The open cookbook for top-tier code large language models. 2024. URL <https://arxiv.org/pdf/2411.04905>.
- Jiang, G., Quan, G., Ding, Z., Luo, Z., Wang, D., and Hu, Z. Flashthink: An early exit method for efficient reasoning, 2025. URL <https://arxiv.org/abs/2505.13949>.
- Jiang, H., Wu, Q., Luo, X., Li, D., Lin, C.-Y., Yang, Y., and Qiu, L. LongLLMLingua: Accelerating and enhancing LLMs in long context scenarios via prompt compression. In *ICLR 2024 Workshop on Mathematical and Empirical Understanding of Foundation Models*, 2024. URL <https://openreview.net/forum?id=9YvfRrpyw>.
- Jung, H. and Kim, K.-J. Discrete prompt compression with reinforcement learning. *IEEE Access*, 12:72578–72587, 2024. ISSN 2169-3536. doi: 10.1109/access.2024.3403426. URL <http://dx.doi.org/10.1109/ACCESS.2024.3403426>.
- Kang, Y., Sun, X., Chen, L., and Zou, W. C3ot: Generating shorter chain-of-thought without compromising effectiveness. *Proceedings of the AAAI Conference on Artificial Intelligence*, 39(23):24312–24320, Apr. 2025a. doi: 10.1609/aaai.v39i23.34608. URL <https://ojs.aaai.org/index.php/AAAI/article/view/34608>.
- Kang, Z., Zhao, X., and Song, D. Scalable best-of-n selection for large language models via self-certainty, 2025b. URL <https://arxiv.org/abs/2502.18581>.
- Kwon, W., Li, Z., Zhuang, S., Sheng, Y., Zheng, L., Yu, C. H., Gonzalez, J. E., Zhang, H., and Stoica, I. Efficient memory management for large language model serving with pagedattention. In *Proceedings of the ACM SIGOPS 29th Symposium on Operating Systems Principles*, 2023.
- Lee, C., Rush, A. M., and Vafa, K. Critical thinking: Which kinds of complexity govern optimal reasoning length?, 2025. URL <https://arxiv.org/abs/2504.01935>.
- Lightman, H., Kosaraju, V., Burda, Y., Edwards, H., Baker, B., Lee, T., Leike, J., Schulman, J., Sutskever, I., and Cobbe, K. Let’s verify step by step. In *ICLR*, 2024. URL <https://openreview.net/forum?id=v8L0pN6EOi>.
- Liu, A. H., Khandelwal, K., Subramanian, S., Jouault, V., Rastogi, A., Sadé, A., Jeffares, A., Jiang, A., Cahill, A., Gavaudan, A., Sablayrolles, A., Héliou, A., You, A., Ehrenberg, A., Lo, A., Eliseev, A., Calvi, A., Sooriyarachchi, A., Bout, B., Rozière, B., Monicault, B. D., Lanfranchi, C., Barreau, C., Courtot, C., Grattarola, D., Dabert, D., de las Casas, D., Chane-Sane, E., Ahmed, F., Berrada, G., Ecrepont, G., Guinet, G., Novikov, G., Kunsch, G., Lample, G., Martin, G., Gupta, G., Ludziejewski, J., Rute, J., Studnia, J., Amar, J., Delas, J., Roberts, J. S., Yadav, K., Chandu, K., Jain, K., Aitchison, L., Fainsin, L., Blier, L., Zhao, L., Martin, L., Saulnier, L., Gao, L., Buyl, M., Jennings, M., Pellat, M., Prins, M., Poirée, M., Guillaumin, M., Dinot, M., Futral, M., Darrin, M., Augustin, M., Chiquier, M., Schimpf, M., Grinsztajn, N., Gupta, N., Raghuraman, N., Bousquet, O., Duchenne, O., Wang, P., von Platen, P., Jacob, P., Wambergue, P., Kurylowicz, P., Muddireddy, P. R., Chagniot, P., Stock, P., Agrawal, P., Torroba, Q., Sauvestre, R., Soletskyi, R., Menneer, R., Vaze, S., Barry, S., Gandhi, S., Waghjale, S., Gandhi, S., Ghosh, S., Mishra, S., Aithal, S., Antoniak, S., Scao, T. L., Cachet, T., Sorg, T. S., Lavril, T., Saada, T. N., Chabal, T., Foubert, T., Robert, T., Wang, T., Lawson, T., Bewley, T., Bewley, T., Edwards, T., Jamil, U., Tomasini, U., Nemychnikova, V., Phung, V., Maladière, V., Richard, V., Bouaziz, W., Li, W.-D., Marshall, W., Li, X., Yang, X., Ouahidi, Y. E., Wang, Y., Tang, Y., and Ramzi, Z. Ministral 3, 2026. URL <https://arxiv.org/abs/2601.08584>.

- Liu, X. and Wang, L. Answer convergence as a signal for early stopping in reasoning, 2025. URL <https://arxiv.org/abs/2506.02536>.
- Lou, C., Sun, Z., Liang, X., Qu, M., Shen, W., Wang, W., Li, Y., Yang, Q., and Wu, S. Adacot: Pareto-optimal adaptive chain-of-thought triggering via reinforcement learning, 2025. URL <https://arxiv.org/abs/2505.11896>.
- Luck, S. J. *An introduction to the event-related potential technique / Steven J. Luck*. The MIT Press, Cambridge, Massachusetts, second edition. edition, 2014. ISBN 0-262-32406-7.
- Luo, H., Shen, L., He, H., Wang, Y., Liu, S., Li, W., Tan, N., Cao, X., and Tao, D. O1-pruner: Length-harmonizing fine-tuning for o1-like reasoning pruning, 2025. URL <https://arxiv.org/abs/2501.12570>.
- Ma, W., He, J., Snell, C., Griggs, T., Min, S., and Zaharia, M. Reasoning models can be effective without thinking, 2025a. URL <https://arxiv.org/abs/2504.09858>.
- Ma, X., Wan, G., Yu, R., Fang, G., and Wang, X. CoT-valve: Length-compressible chain-of-thought tuning. In Che, W., Nabende, J., Shutova, E., and Pilehvar, M. T. (eds.), *Proceedings of the 63rd Annual Meeting of the Association for Computational Linguistics (Volume 1: Long Papers)*, pp. 6025–6035, Vienna, Austria, July 2025b. Association for Computational Linguistics. ISBN 979-8-89176-251-0. doi: 10.18653/v1/2025.acl-long.300. URL <https://aclanthology.org/2025.acl-long.300/>.
- Mao, M., Yin, B., Zhu, Y., and Fang, X. Early stopping chain-of-thoughts in large language models, 2025. URL <https://arxiv.org/abs/2509.14004>.
- Mu, J., Li, X. L., and Goodman, N. Learning to compress prompts with gist tokens. In *Thirty-seventh Conference on Neural Information Processing Systems*, 2023. URL <https://openreview.net/forum?id=2DtXPCL3T5>.
- Muennighoff, N., Yang, Z., Shi, W., Li, X. L., Fei-Fei, L., Hajishirzi, H., Zettlemoyer, L., Liang, P., Candès, E., and Hashimoto, T. s1: Simple test-time scaling, 2025. URL <https://arxiv.org/abs/2501.19393>.
- Nagle, A., Girish, A., Bondaschi, M., Gastpar, M., Makkuva, A. V., and Kim, H. Fundamental limits of prompt compression: A rate-distortion framework for black-box language models. In Globerson, A., Mackey, L., Belgrave, D., Fan, A., Paquet, U., Tomczak, J., and Zhang, C. (eds.), *Advances in Neural Information Processing Systems*, volume 37, pp. 94934–94970. Curran Associates, Inc., 2024. doi: 10.52202/079017-3009. URL https://proceedings.neurips.cc/paper_files/paper/2024/file/ac8fbbba029dadca99d6b8c3f913d3ed6-Paper-Conference.pdf.
- NVIDIA. OpenScience dataset (v1). <https://huggingface.co/datasets/nvidia/OpenScience>, 2025. Last updated: June 18 (per repository history). Accessed: 2026-01-07.
- OpenAI. Learning to reason with llms. <https://openai.com/index/learning-to-reason-with-llms/>, September 12 2024. Accessed: 2025-01-19.
- Pan, Z., Wu, Q., Jiang, H., Xia, M., Luo, X., Zhang, J., Lin, Q., Ruhle, V., Yang, Y., Lin, C.-Y., Zhao, H. V., Qiu, L., and Zhang, D. LLMingua-2: Data distillation for efficient and faithful task-agnostic prompt compression. In Ku, L.-W., Martins, A., and Srikumar, V. (eds.), *Findings of the Association for Computational Linguistics ACL 2024*, pp. 963–981, Bangkok, Thailand and virtual meeting, August 2024. Association for Computational Linguistics. URL <https://aclanthology.org/2024.findings-acl.57>.
- Qian, C., Liu, D., Wen, H., Bai, Z., Liu, Y., and Shao, J. Demystifying reasoning dynamics with mutual information: Thinking tokens are information peaks in llm reasoning. *arXiv preprint arXiv:2506.02867*, 2025.
- Qin, G., Rosset, C., Chau, E., Rao, N., and Van Durme, B. Dodo: Dynamic contextual compression for decoder-only LMs. In Ku, L.-W., Martins, A., and Srikumar, V. (eds.), *Proceedings of the 62nd Annual Meeting of the Association for Computational Linguistics (Volume 1: Long Papers)*, pp. 9961–9975, Bangkok, Thailand, August 2024. Association for Computational Linguistics. doi: 10.18653/v1/2024.acl-long.536. URL <https://aclanthology.org/2024.acl-long.536/>.
- Rein, D., Hou, B. L., Stickland, A. C., Petty, J., Pang, R. Y., Dirani, J., Michael, J., and Bowman, S. R. GPQA: A graduate-level google-proof q&a benchmark. In *First Conference on Language Modeling*, 2024. URL <https://openreview.net/forum?id=Ti67584b98>.
- Schuster, T., Fisch, A., Gupta, J., Dehghani, M., Bahri, D., Tran, V., Tay, Y., and Metzler, D. Confident adaptive language modeling. In Koyejo, S., Mohamed, S., Agarwal, A., Belgrave, D., Cho, K., and Oh, A. (eds.), *Advances in Neural Information Processing Systems*, volume 35, pp. 17456–17472. Curran Associates, Inc., 2022. URL https://proceedings.neurips.cc/paper_files/paper/2022/file/

- 6fac9e316a4ae75ea244ddcef1982c71-Paper-Conclusion.pdf.
- Shrivastava, V., Awadallah, A., Balachandran, V., Garg, S., Behl, H., and Papailiopoulos, D. Sample more to think less: Group filtered policy optimization for concise reasoning, 2025. URL <https://arxiv.org/abs/2508.09726>.
- Wang, C., Feng, Y., Chen, D., Chu, Z., Krishna, R., and Zhou, T. Wait, we don't need to "wait"! removing thinking tokens improves reasoning efficiency. In Christodoulopoulos, C., Chakraborty, T., Rose, C., and Peng, V. (eds.), *Findings of the Association for Computational Linguistics: EMNLP 2025*, pp. 7459–7482, Suzhou, China, November 2025a. Association for Computational Linguistics. ISBN 979-8-89176-335-7. doi: 10.18653/v1/2025.findings-emnlp.394. URL <https://aclanthology.org/2025.findings-emnlp.394/>.
- Wang, X., McInerney, J., Wang, L., and Kallus, N. Entropy after $\langle /Think \rangle$ for reasoning model early exiting, 2025b. URL <https://arxiv.org/abs/2509.26522>.
- Wu, M., Zhou, C., Bates, S., and Jaakkola, T. Thought calibration: Efficient and confident test-time scaling. In Christodoulopoulos, C., Chakraborty, T., Rose, C., and Peng, V. (eds.), *Proceedings of the 2025 Conference on Empirical Methods in Natural Language Processing*, pp. 14302–14316, Suzhou, China, November 2025a. Association for Computational Linguistics. ISBN 979-8-89176-332-6. doi: 10.18653/v1/2025.emnlp-main.722. URL <https://aclanthology.org/2025.emnlp-main.722/>.
- Wu, Y., Wang, Y., Du, T., Jegelka, S., and Wang, Y. When more is less: Understanding chain-of-thought length in LLMs. In *Workshop on Reasoning and Planning for Large Language Models*, 2025b. URL <https://openreview.net/forum?id=W8dxn7hBk0>.
- Xia, H., Leong, C. T., Wang, W., Li, Y., and Li, W. TokenSkip: Controllable chain-of-thought compression in LLMs. In Christodoulopoulos, C., Chakraborty, T., Rose, C., and Peng, V. (eds.), *Proceedings of the 2025 Conference on Empirical Methods in Natural Language Processing*, pp. 3351–3363, Suzhou, China, November 2025. Association for Computational Linguistics. ISBN 979-8-89176-332-6. doi: 10.18653/v1/2025.emnlp-main.165. URL <https://aclanthology.org/2025.emnlp-main.165/>.
- Yang, A., Li, A., Yang, B., Zhang, B., Hui, B., Zheng, B., Yu, B., Gao, C., Huang, C., Lv, C., Zheng, C., Liu, D., Zhou, F., Huang, F., Hu, F., Ge, H., Wei, H., Lin, H., Tang, J., Yang, J., Tu, J., Zhang, J., Yang, J., Yang, J., Zhou, J., Zhou, J., Lin, J., Dang, K., Bao, K., Yang, K., Yu, L., Deng, L., Li, M., Xue, M., Li, M., Zhang, P., Wang, P., Zhu, Q., Men, R., Gao, R., Liu, S., Luo, S., Li, T., Tang, T., Yin, W., Ren, X., Wang, X., Zhang, X., Ren, X., Fan, Y., Su, Y., Zhang, Y., Zhang, Y., Wan, Y., Liu, Y., Wang, Z., Cui, Z., Zhang, Z., Zhou, Z., and Qiu, Z. Qwen3 technical report, 2025a. URL <https://arxiv.org/abs/2505.09388>.
- Yang, C., Si, Q., Duan, Y., Zhu, Z., Zhu, C., Li, Q., Chen, M., Lin, Z., and Wang, W. Dynamic early exit in reasoning models, 2025b. URL <https://arxiv.org/abs/2504.15895>.
- Yang, R., Bai, H., Liu, S., Yu, G., Fan, R., Dang, Y., Zhang, J., Liu, K., Zhu, J., and Chen, P. Specexit: Accelerating large reasoning model via speculative exit, 2025c. URL <https://arxiv.org/abs/2509.24248>.
- Yi, J., Wang, J., and Li, S. Shorterbetter: Guiding reasoning models to find optimal inference length for efficient reasoning. In *The Thirty-ninth Annual Conference on Neural Information Processing Systems*, 2025. URL <https://openreview.net/forum?id=MJvwm5dBZM>.
- Zhang, A., Chen, Y., Pan, J., Zhao, C., Panda, A., Li, J., and He, H. Reasoning models know when they're right: Probing hidden states for self-verification. In *Second Conference on Language Modeling*, 2025a. URL <https://openreview.net/forum?id=06I0Av7683>.
- Zhang, J., Lin, N., Hou, L., Feng, L., and Li, J. Adapt-Think: Reasoning models can learn when to think. In Christodoulopoulos, C., Chakraborty, T., Rose, C., and Peng, V. (eds.), *Proceedings of the 2025 Conference on Empirical Methods in Natural Language Processing*, pp. 3716–3730, Suzhou, China, November 2025b. Association for Computational Linguistics. ISBN 979-8-89176-332-6. doi: 10.18653/v1/2025.emnlp-main.184. URL <https://aclanthology.org/2025.emnlp-main.184/>.
- Zhang, J., Zhu, Y., Sun, M., Luo, Y., Qiao, S., Du, L., Zheng, D., Chen, H., and Zhang, N. LightThinker: Thinking step-by-step compression. In Christodoulopoulos, C., Chakraborty, T., Rose, C., and Peng, V. (eds.), *Proceedings of the 2025 Conference on Empirical Methods in Natural Language Processing*, pp. 13307–13328, Suzhou, China, November 2025c. Association for Computational Linguistics. ISBN 979-8-89176-332-6. doi: 10.18653/v1/2025.emnlp-main.673. URL <https://aclanthology.org/2025.emnlp-main.673/>.
- Zhang, Z., He, X., Yan, W., Shen, A., Zhao, C., Wang, S., Shen, Y., and Wang, X. E. Soft thinking: Unlocking the reasoning potential of llms in continuous

concept space, 2025d. URL <https://arxiv.org/abs/2505.15778>.

Algorithm 1 Answer Span Extraction, Identification, and Verification With Feedback

```

1: Input: CoT  $r$ , final solution  $s$ , LRM, tokenizer, max retries  $K$ 
2: Output: answer position  $i^*$  (token index where answer is reached)
3:
4: // Extract final answer value from model output
5:  $\hat{a} \leftarrow \text{LRM}(\text{"Extract the final answer from: " } + s)$ 
6:
7: // Iteratively extract and verify span with feedback
8:  $z \leftarrow \emptyset$  // feedback provided to the LRM
9: for  $k = 1, \dots, K$  do
10: // Ask LRM to identify a string span containing the first occurrence of  $\hat{a}$  in  $r$ 
11:  $d \leftarrow \text{LRM}(\text{"Find first occurrence of " } + \hat{a} + \text{" in: " } + r + z)$ 
12:
13: // Verify the identified span contains the answer
14:  $v \leftarrow \text{LRM}(\text{"Does " } + d + \text{" contain " } + \hat{a} + \text{"?"})$ 
15:
16: if  $v == \text{true}$  then
17:   break // span verified, proceed
18: end if
19:
20:  $z \leftarrow z + \text{"\n Previous span " } + d + \text{" was incorrect, try again"}$ 
21: end for
22:
23: // Pattern match span text to get character-wise positioning of the span
24:  $c \leftarrow \text{FuzzyMatch}(d, r)$  //  $c$  is an integer-based character index of  $d$  in  $r$ 
25:
26: // Convert to token position where answer is reached
27:  $i^* \leftarrow \text{CharToTokenPos}(c + \text{len}(d), r, \text{tokenizer})$ 
28:
29: return  $i^*$ 

```

A. Additional Details on Our Methods

A.1. Early Answer Extraction, Identification, and Verification

Algorithm 1 contains pseudocode for our pipeline. i^* , the index of the earliest token position containing \hat{a} , is used to construct the label set of our training data by setting all positions prior to i^* to 0 and setting all positions after i^* to 1. Each of the three steps (extraction, identification, and verification) requires separate calls to an LRM; please refer to our codebase for details on the exact system prompts that we used for each step.

A.2. Training Dataset Details

Our training dataset consists of CoTs from AIME (1983–2024) ([Art of Problem Solving](#)), MATH ([Lightman et al., 2024](#)), OpenCoder-SFT ([Huang et al., 2024](#)), and OpenScience ([NVIDIA, 2025](#)). All 933 samples and all 12,000 samples from the AIME (1983–2024) and MATH datasets, respectively, are used. We randomly select 12,000 samples from the `educational_instruct` subset of the OpenCoder-SFT-Stage2 dataset, which we refer to as “OpenCoder-SFT” in the main paper. This subset consists of generated and validated Python coding examples. Our sampling procedure for this dataset was not uniform, unlike the others. Instead, problems are grouped by their `entry_point` field, and sampling is split into rounds, with each round randomly sampling one problem from that group without replacement. Finally, we randomly sample an additional 12,000 samples from the `OS-Q3-235B-4` subset of the OpenScience dataset. This subset consists of multiple-choice STEM question-answer pairs that were synthetically generated from Qwen3-235B-A22B ([Yang et al., 2025a](#)).

Three CoTs are sampled per problem by the target LRM (we used Qwen and Mistral models), yielding a set of approximately

110,799 CoTs per LRM. The respective answer positions for each set of CoTs is obtained with our extraction method outlined in Sec. 4.1. However, this procedure is not perfect, as even with our retry logic, the answer extractor, identifier, and verifier LRM (Qwen3-30B-A3B-Thinking-2507) cannot always identify the earliest final answer position. Thus, all three of these steps are successful for roughly 70%–80% of CoTs. Finally, a training-ready dataset for each LRM is formed by preparing label vectors (based on the answer positions), loss masks (based on the positions of `<think>` and `</think>`), and tokenizing the CoTs.

A.3. Implementation of the Baseline Methods

Dynasor. Dynasor (Fu et al., 2025a) works by interrupting reasoning at regular token intervals (e.g. every 32, or 64 tokens) by injecting the prompt “Oh, I suddenly got the answer to the whole problem, Final Answer: boxed{” to extract the model’s current answer. The method decides to exit early when consistent answers appear across multiple probing intervals for at least w times. In our experiments, we set $w=8$ and use a token interval of 64 tokens, following their so-called *mild* configuration setup.

Thought Calibration. (Wu et al., 2025a) propose training a linear probe to predict optimal stopping points during reasoning generation. The method first segments reasoning trajectories (CoTs) into individual steps, delimited by “\n\n” and containing words like “wait” or “but”. Three probe variants are introduced: *Supervised* predicts whether the LRM is correct based on current thoughts; *Consistent* predicts whether the current answer (\hat{a}) matches the final answer (a); and *Novel Leaf* predicts whether the current step is a leaf node but not novel.

The stopping decision is controlled by two hyperparameters: *tolerance* δ (the maximum acceptable risk of stopping incorrectly) that implies a threshold λ (the calibrated probe score cutoff that triggers stopping), and *window size* (the number of consecutive reasoning steps averaged to smooth predictions before threshold comparison). We retrain the *Supervised* and *Consistent* probes on the S1-K dataset (Muennighoff et al., 2025) for all four models in our experiments: Qwen3-8B, Qwen3-14B, Ministral-3-8B-Reasoning-2512, and Ministral-3-8B-Reasoning-2512. For inference, we use the hyperparameters specified in Table 3. As shown in Table 3, the Qwen3 models require lower thresholds compared to the Ministral models, as their probe outputs yield systematically lower confidence scores. Similar model-specific calibration requirements have been observed in prior work (Yang et al., 2025b).

| Model | Supervised | | | Consistent | | |
|--------------------------------|------------------------|-------------------------|-------------|------------------------|-------------------------|-------------|
| | tolerance (δ) | threshold (λ) | window size | tolerance (δ) | threshold (λ) | window size |
| Qwen3-8B | 0.25 | 0.6526 | 10 | 0.25 | 0.8790 | 10 |
| Qwen3-14B | 0.25 | 0.6377 | 10 | 0.25 | 0.8679 | 10 |
| Ministral-3-8B-Reasoning-2512 | 0.10 | 0.8173 | 10 | 0.025 | 0.9973 | 10 |
| Ministral-3-14B-Reasoning-2512 | 0.10 | 0.8306 | 10 | 0.025 | 0.9973 | 10 |

Table 3. Hyperparameters used for *Supervised* and *Consistent* linear probs for Thought Calibration.

We reported the results for the *Supervised* probe in Table 1, as it performed better across test datasets than the *Consistent* probe. For comparison, we report the results for both probes in Table 4. Note that for the *Consistent* probe with Ministral models, tolerance 0.025 represents the smallest feasible setting among values suggested in (Wu et al., 2025a). The smallest possible setting, being tolerance 0.01, yields threshold=1.0, resulting in no compression.

| Model | MATH-500 | | AIME 2025 | | GPQA | | HumanEval | |
|--------------------------------|--------------------|---------------------|--------------------|---------------------|--------------------|---------------------|--------------------|---------------------|
| | Acc (\uparrow) | CR (\downarrow) | Acc (\uparrow) | CR (\downarrow) | Acc (\uparrow) | CR (\downarrow) | Acc (\uparrow) | CR (\downarrow) |
| <i>Supervised</i> | | | | | | | | |
| Qwen3-8B | 90.1% | 93.89% | 65.8% | 81.54% | 52.6% | 78.87% | 71.8% | 92.92% |
| Qwen3-14B | 89.8% | 91.92% | 63.3% | 71.29% | 54.6% | 81.90% | 74.8% | 87.12% |
| Ministral-3-8B-Reasoning-2512 | 87.7% | 87.80% | 83.7% | 91.16% | 47.3% | 71.78% | 47.2% | 87.16% |
| Ministral-3-14B-Reasoning-2512 | 87.3% | 95.86% | 59.4% | 79.77% | 49.5% | 73.81% | 27.6% | 96.25% |
| <i>Consistent</i> | | | | | | | | |
| Qwen3-8B | 88.2% | 72.09% | 43.1% | 54.64% | 44.7% | 45.17% | 70.7% | 73.90% |
| Qwen3-14B | 85.9% | 64.40% | 41.7% | 45.57% | 48.3% | 53.83% | 70.9% | 39.60% |
| Ministral-3-8B-Reasoning-2512 | 75.8% | 80.53% | 23.3% | 60.50% | 42.4% | 62.69% | 34.2% | 75.24% |
| Ministral-3-14B-Reasoning-2512 | 68.7% | 77.40% | 9.4% | 34.42% | 40.6% | 59.97% | 9.6% | 95.90% |

Table 4. Performance comparison of *Supervised* and *Consistent* probes for Thought Calibration across models and tasks.

B. Additional Experimental Results

Event-Locked Averaging Token-Confidence. Figs. 10 to 13 show the Token-Confidence and log-probabilities for the single-sample and event-locked averaging case, similar to what’s shown in Fig. 2, separately for each data source. While the exact contours of these two signal types vary for different data sources, the same idea applies to all: the LRM’s Token-Confidence has a sharp spike at the position of the first occurrence of \hat{a} , followed by a sharp decrease. In all cases, the Token-Confidence then has a quick recovery before plateauing or decaying.

Token Usage Frequency Shift. Fig. 14 shows an expanded view of Fig. 3, including six additional “thinking tokens.” Figs. 15 to 18 reproduces this expanded plot, but with the data sources separated. Interestingly, the occurrence rates can vary substantially across different data sources. For example, for the token `alternatively`, only 19.2% of points lie above the diagonal (only 19.2% of CoTs have the token `alternatively` occurring more frequently after the answer than before), and 45.8% (nearly half!) of the points are at the origin (the token `alternatively` never occurs in 45.8% of CoTs) for OpenCoder-SFT. However, for MATH, 80.4% of points lie above the diagonal and only 4.1% lie at the origin for the same token. Other tokens, like `therefore`, are strongly biased toward occurring after the answer.

Fig. 19 shows that the average occurrence rate across CoTs from all data sources changes depending on how long the CoT is. We normalize by the number of tokens occurring before and after the first occurrence of \hat{a} for the before and after rates, respectively, so these plots suggest that the LRM uses `hmm`, `okay`, and `another` more frequently for shorter CoTs than longer ones.

TERMINATOR Predictions During Reasoning. Fig. 20 shows the event-locked average of the predicted probabilities from TERMINATOR for each data source, and Fig. 21, Fig. 22, Fig. 23, and Fig. 24 show the predicted probabilities from four randomly chosen examples for AIME25, MATHH-500, HumanEval, and GPQA, respectively. The event-locked average and the individual examples from MATH-500 and HumanEval show sharp transitions in predicted confidence at the exiting threshold, with good separation (dotted gray line). However, AIME25 and GPQA examples do not show such a sharp transition, suggesting that it is challenging for TERMINATOR to identify a good exit position for very hard tasks.

TERMINATOR Thresholding. Fig. 25 shows how the compression rate and the accuracy change as a result of varying the threshold used by TERMINATOR to predict 0 or 1. For example, a threshold $\tau = 0.7$ requires TERMINATOR to have a predictive confidence of at least 0.7 to predict 1. Interestingly, varying the threshold has a greater impact on compression rate than on accuracy; setting $\tau = 0.1$ yields 8% and 17% better compression rates for MATH-500 and HumanEval, respectively, compared to $\tau = 0.9$, with almost no change in accuracy! However, more challenging datasets, such as AIME25 and GPQA, exhibit notable changes in accuracy as the threshold varies, though the percent drop in accuracy from $\tau = 0.9$ to $\tau = 0.1$ is less than the improvement in compression rate. For example, from $\tau = 0.9$ to $\tau = 0.1$ yields a 6% drop in accuracy but a 27% improvement in the compression rate for GPQA. Since the accuracy drop is so small, this suggests that TERMINATOR is reasonably confident at determining an appropriate exit position on the harder datasets, and that additional reasoning time can only improve accuracy a little.

Answer Prediction Histograms. Fig. 26 gives an overview of the position of the first occurrence of \hat{a} in the CoTs for each data source we used for training. Fig. 27 shows the compression rate statistics of TERMINATOR for each test dataset.

Case Study of TERMINATOR. By manual inspection, we have seen that for easier problems in the MATH-500 dataset, there is a clearer transition to overthinking, which is well detected by TERMINATOR. However, for harder AIME25 problems, the transition is less obvious. Figs. 28 to 31 show the generated CoTs of the Qwen3-14B model for a single sample from MATH-500 and AIME25 with the predicted probabilities from TERMINATOR.

Pareto Frontiers: Accuracy vs. Compression Rate

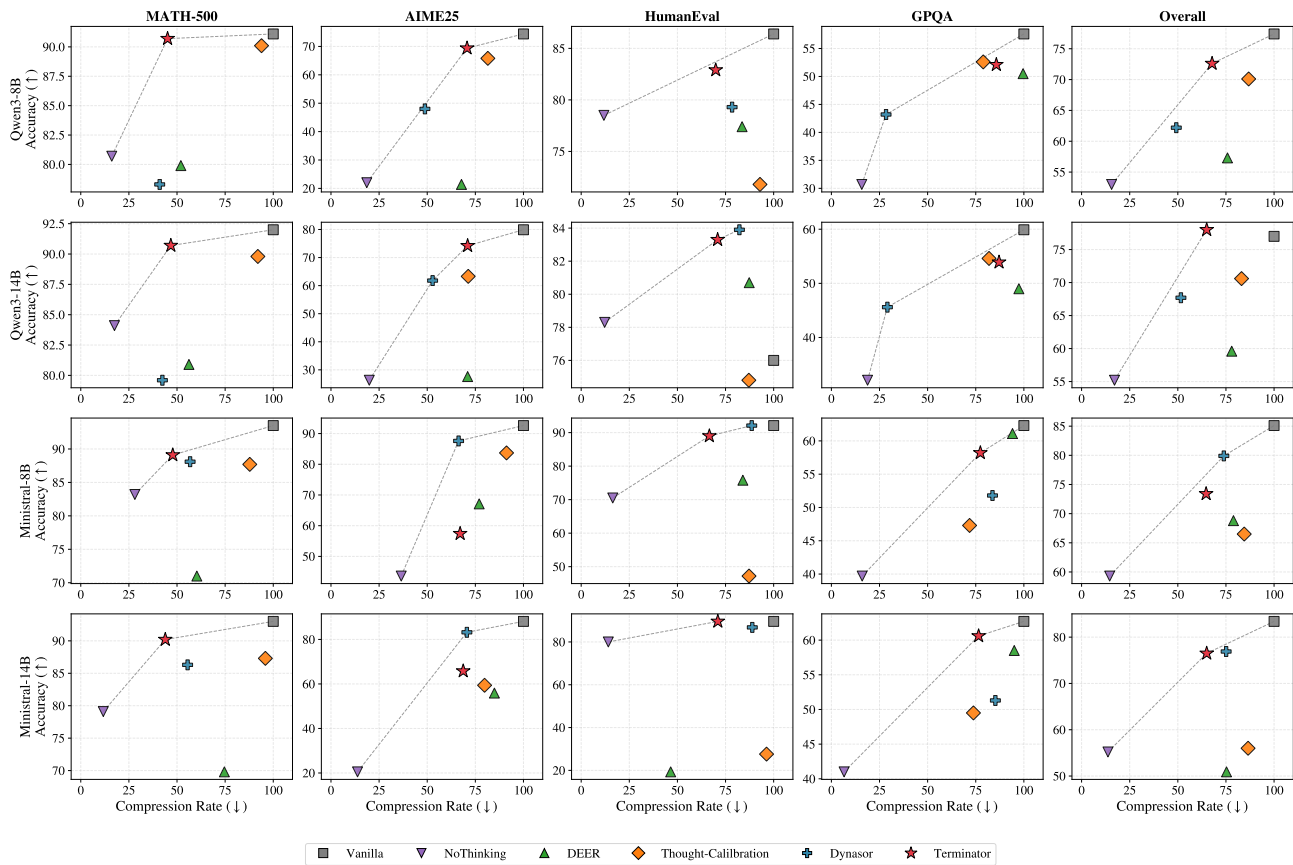


Figure 9. **Pareto Frontier.** TERMINATOR consistently achieves strong Pareto efficiency, reflected by the best accuracy–efficiency tradeoff across models and tasks. Here we plot the Pareto frontiers of accuracy versus compression rate across four reasoning models (Qwen3-8B, Qwen3-14B, Ministral-8B, Ministral-14B) and four benchmarks (MATH-500, AIME25, HumanEval, GPQA). Each point represents a method’s accuracy and compression rate, with lower compression rates indicating greater token savings. The dashed line traces the Pareto frontier connecting non-dominated solutions. The data used to generate this figure is the same as the data from Table 1.

Single Sample and Averaged Time Series for Qwen3-8B - AIME ($n = 800$)

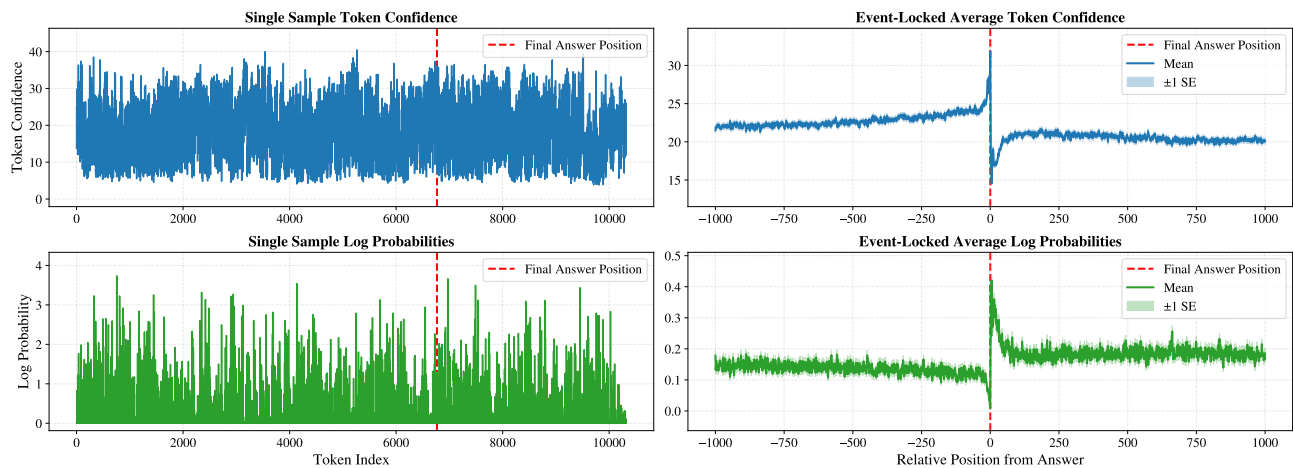


Figure 10. **Event-Locked Averaging of Token-Confidence for AIME (1983–2024).** A reproduction of Fig. 2, but only using CoTs from 800 randomly selected AIME (1983–2024) problems.

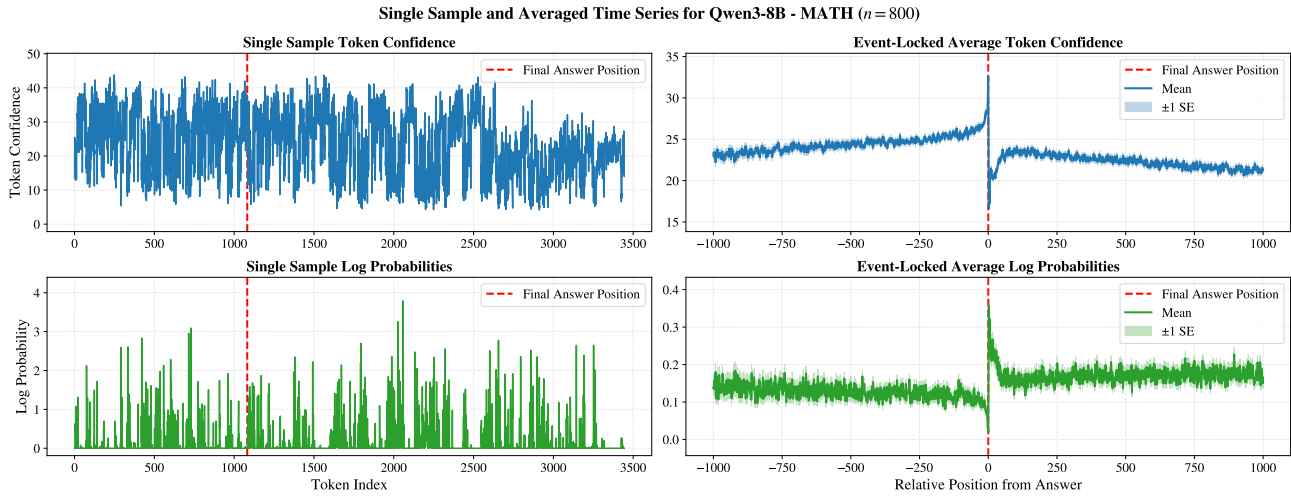


Figure 11. Event-Locked Averaging of Token-Confidence for MATH. A reproduction of Fig. 2, but only using CoTs from 800 randomly selected MATH problems.

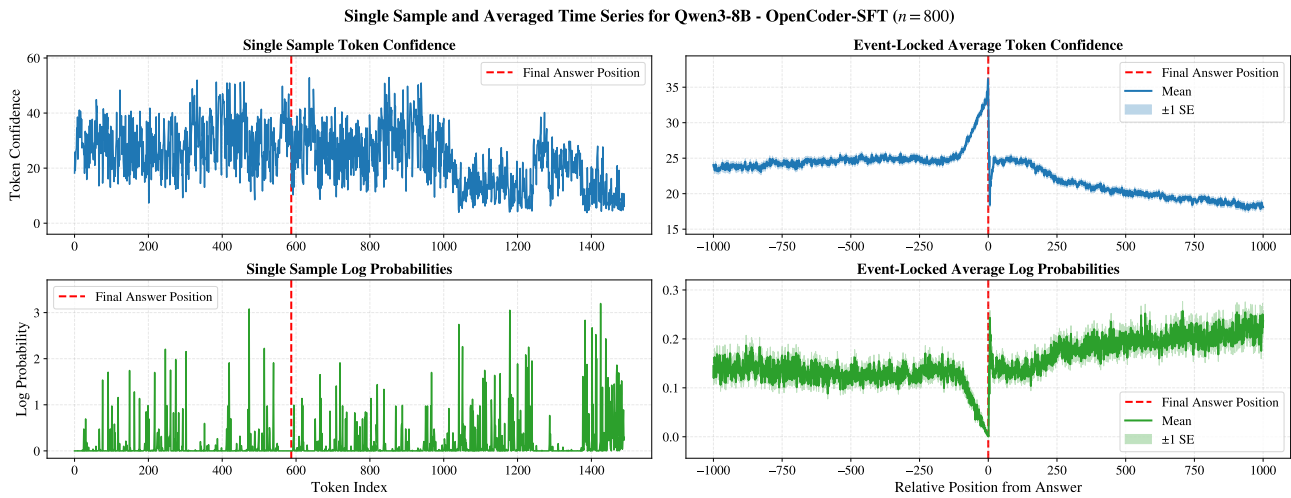


Figure 12. Event-Locked Averaging of Token-Confidence for OpenCoder-SFT. A reproduction of Fig. 2, but only using CoTs from 800 randomly selected OpenCoder-SFT problems.

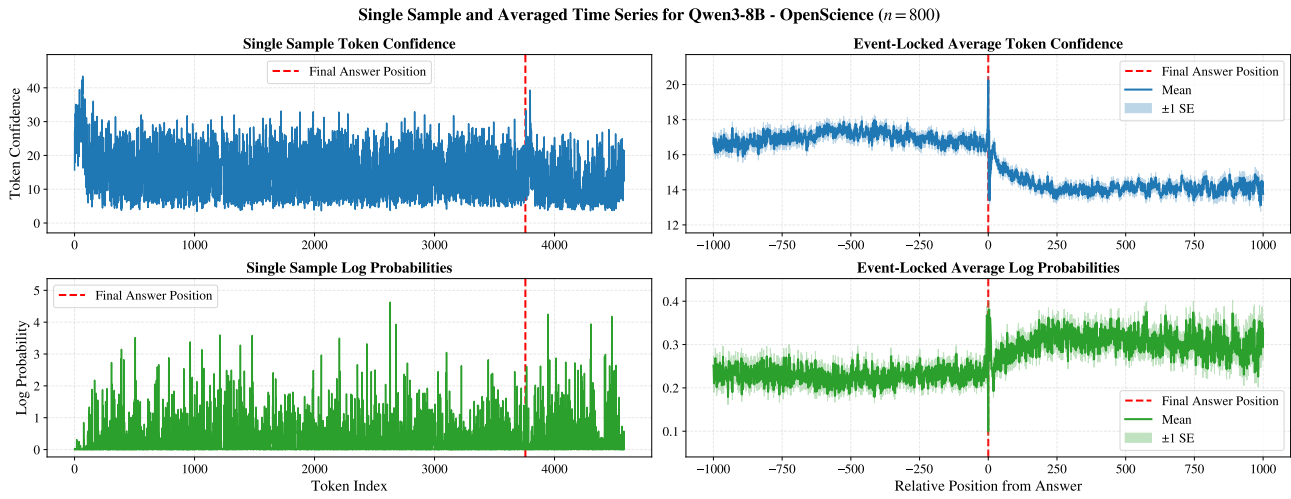


Figure 13. Event-Locked Averaging of Token-Confidence for OpenScience. A reproduction of Fig. 2, but only using CoTs from 800 randomly selected OpenScience problems.

Token Occurrence Ratios for Qwen3-8B - All Data Sources ($n = 3200$)

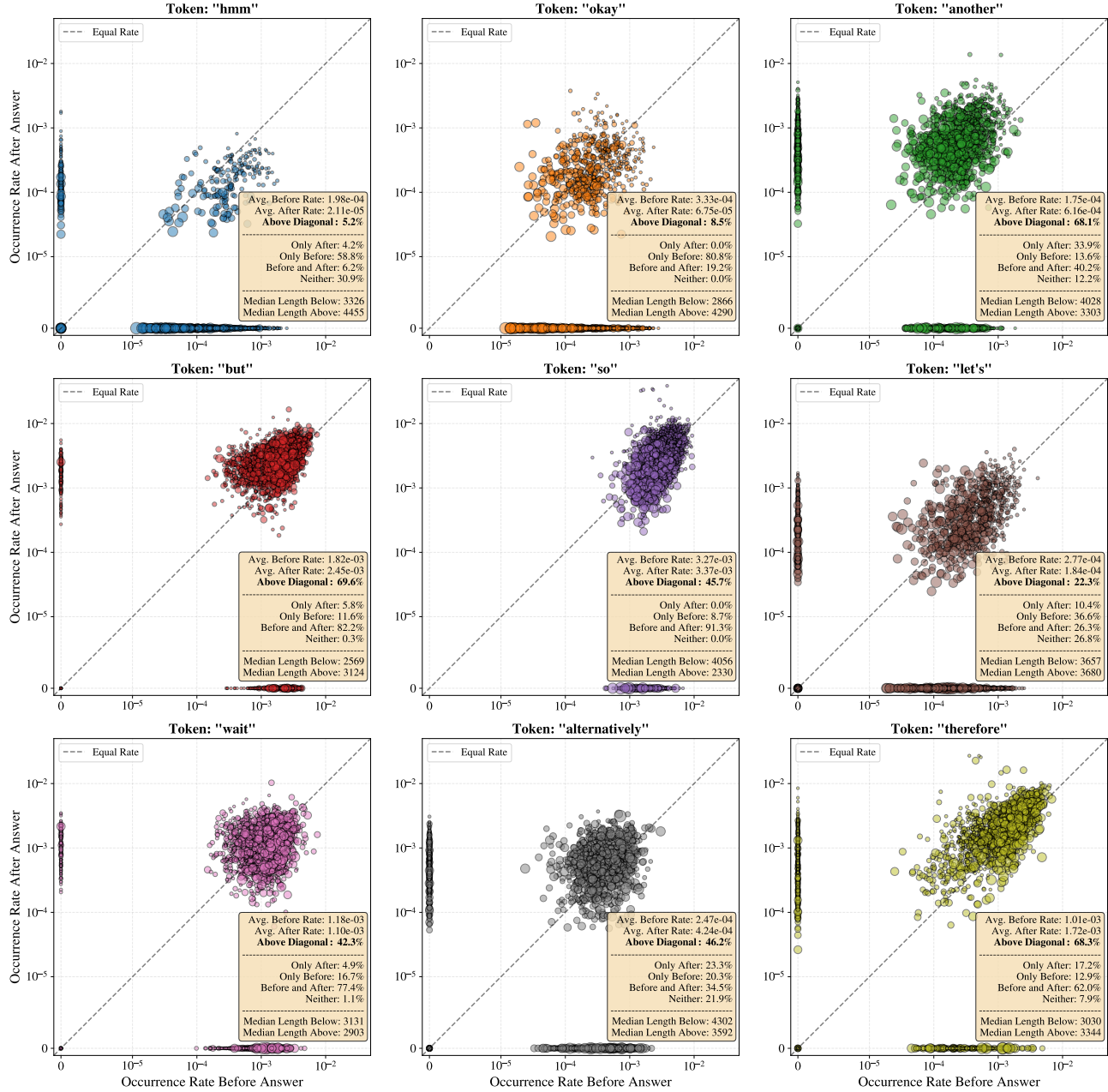


Figure 14. **Token Usage Frequency Shift.** An extension of the results shown in Fig. 3, highlighting additional “thinking tokens.” While most “thinking tokens” shown here have some bias, often occurring before and after the first occurrence of the final answer as indicated by the **Above Diagonal** statistic, some tokens, like “so,” are close to an equal rate on average.

Token Occurrence Ratios for Qwen3-8B - AIME ($n = 800$)

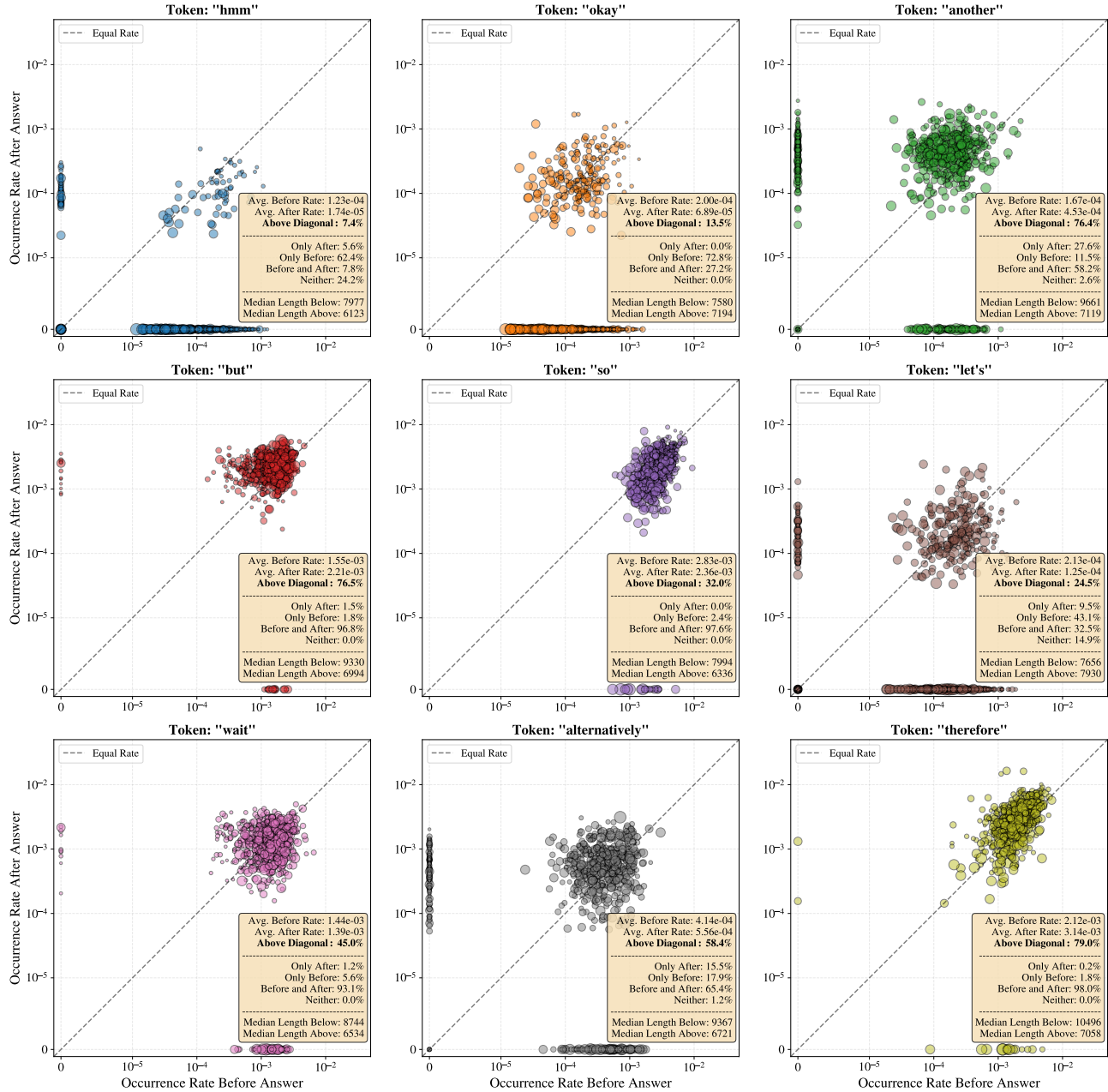


Figure 15. Token Usage Frequency Shift for AIME (1983–2024). A reproduction of Fig. 14, but only using CoTs from 800 randomly selected AIME (1983–2024) problems.

Token Occurrence Ratios for Qwen3-8B - MATH ($n=800$)

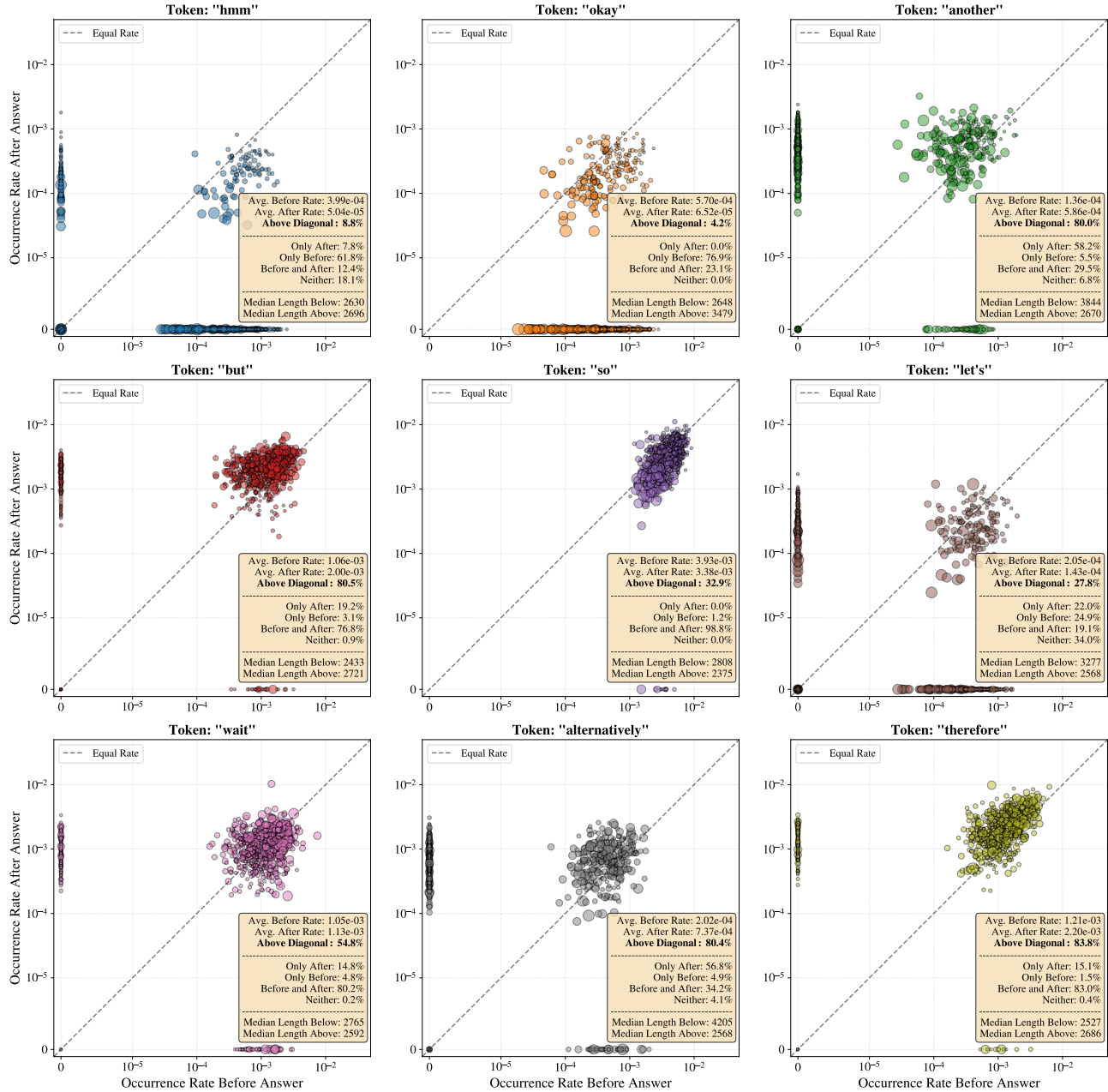


Figure 16. Token Usage Frequency Shift for MATH. A reproduction of Fig. 14, but only using CoTs from 800 randomly selected MATH problems.

Token Occurrence Ratios for Qwen3-8B - OpenCoder-SFT ($n = 800$)

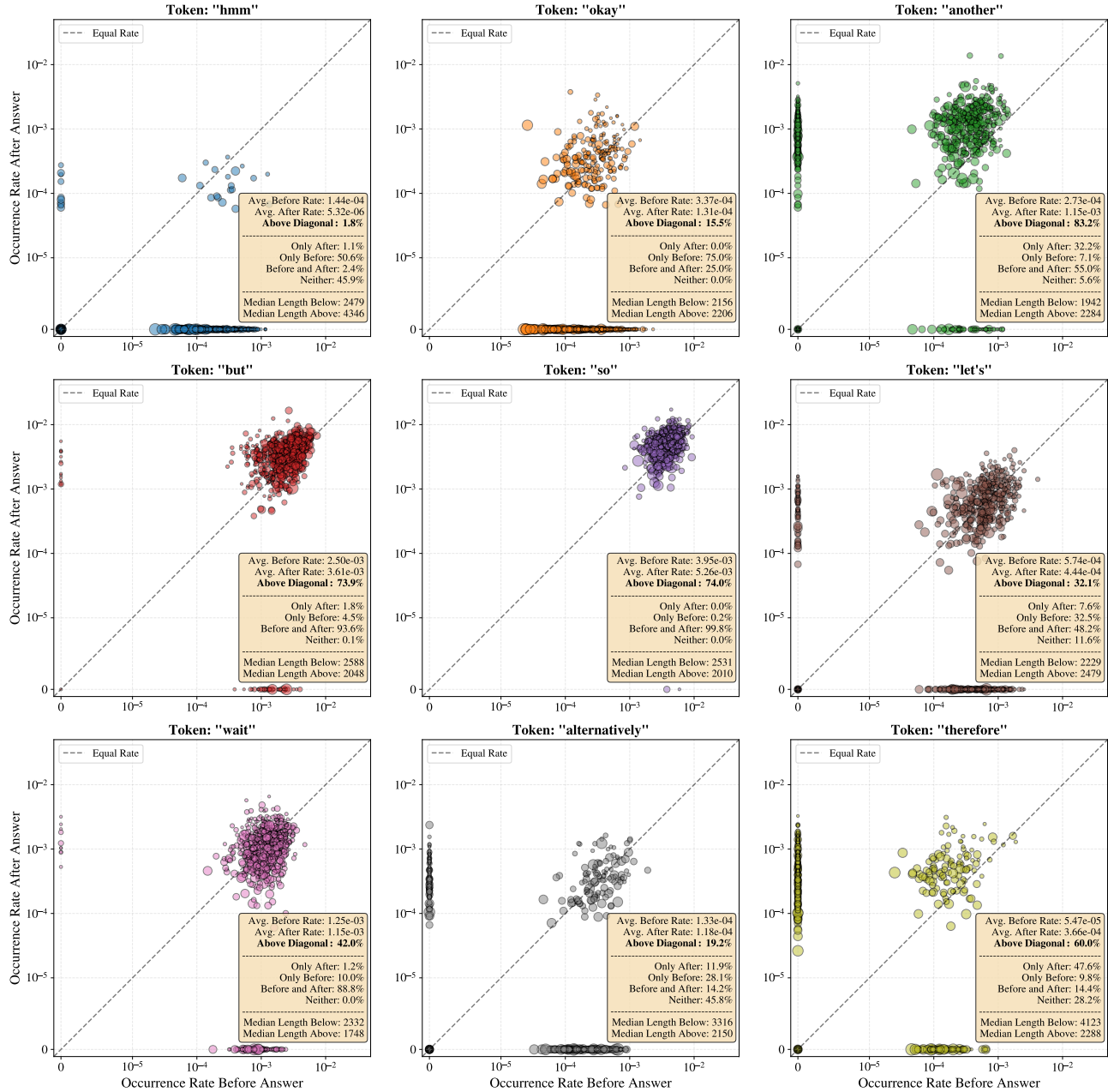


Figure 17. Token Usage Frequency Shift for OpenCoder-SFT. A reproduction of Fig. 14, but only using CoTs from 800 randomly selected OpenCoder-SFT problems.

Token Occurrence Ratios for Qwen3-8B - OpenScience (n = 800)

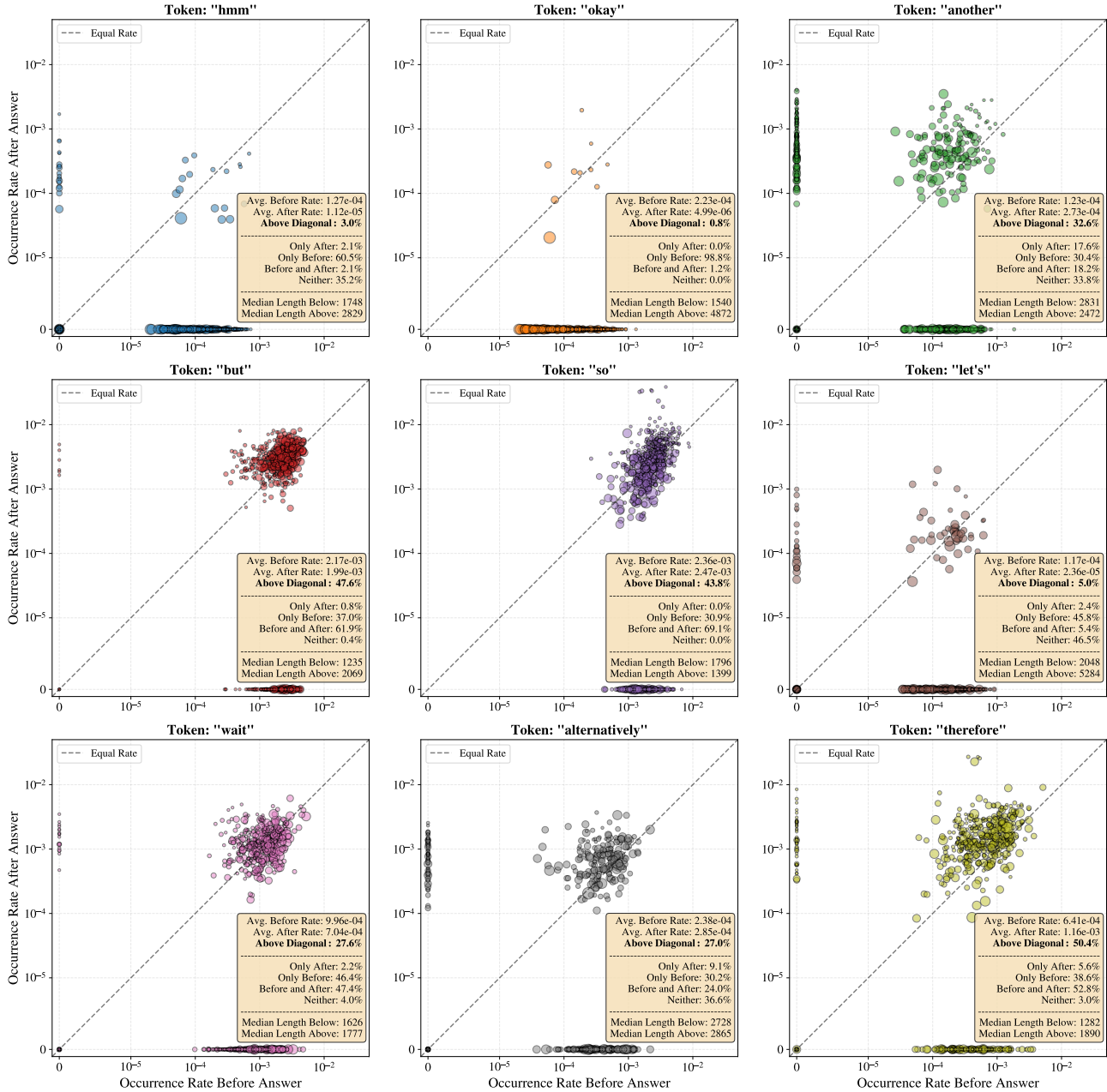


Figure 18. Token Usage Frequency Shift for OpenScience. A reproduction of Fig. 14, but only using CoTs from 800 randomly selected OpenScience problems.

Occurrence Rates vs CoT Length for Qwen3-8B - All Data Sources

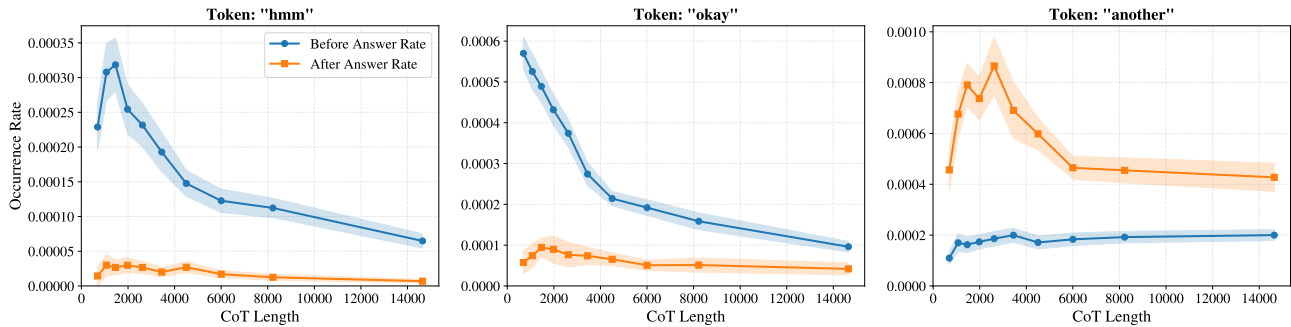


Figure 19. **Token Occurrence Rate vs CoT Length.** For some tokens, such as these three “thinking tokens,” occurrence rates decrease rapidly as CoT length increases. Interestingly, the side of the answer (either “before” or “after”) with the highest rate is the one that decays the most (the “before” rate for *hmm* and *okay* and the “after” rate for *another*), while the side with the lower rate sees only a slight decrease or increase. For each plot, the lengths are placed into ten bins with percentile-based bin edges. In other words, each bin contains approximately 10% of the samples. Shaded regions indicate the 95% confidence interval.

Event-Locked Average Exit Predictions by Data Source for Qwen3-8B

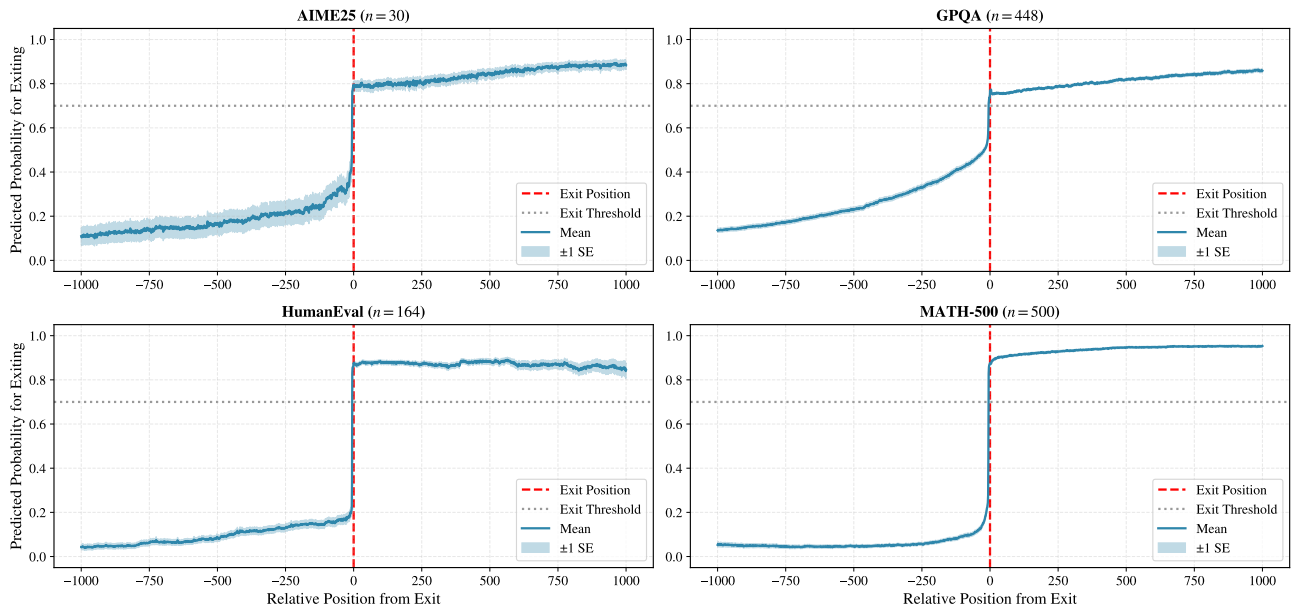


Figure 20. **Predicted Probabilities Event-Locked Averaging.** The dashed vertical line shows where TERMINATOR terminates the CoT with a sliding window of 10 and an exit threshold of 0.7, as indicated by the horizontal dotted line. We show the average predicted probability stream across all test problems from MATH-500, AIME25, HumanEval, and GPQA. Figs. 21 to 24 show predictions streams from individual, randomly drawn samples from each data source.

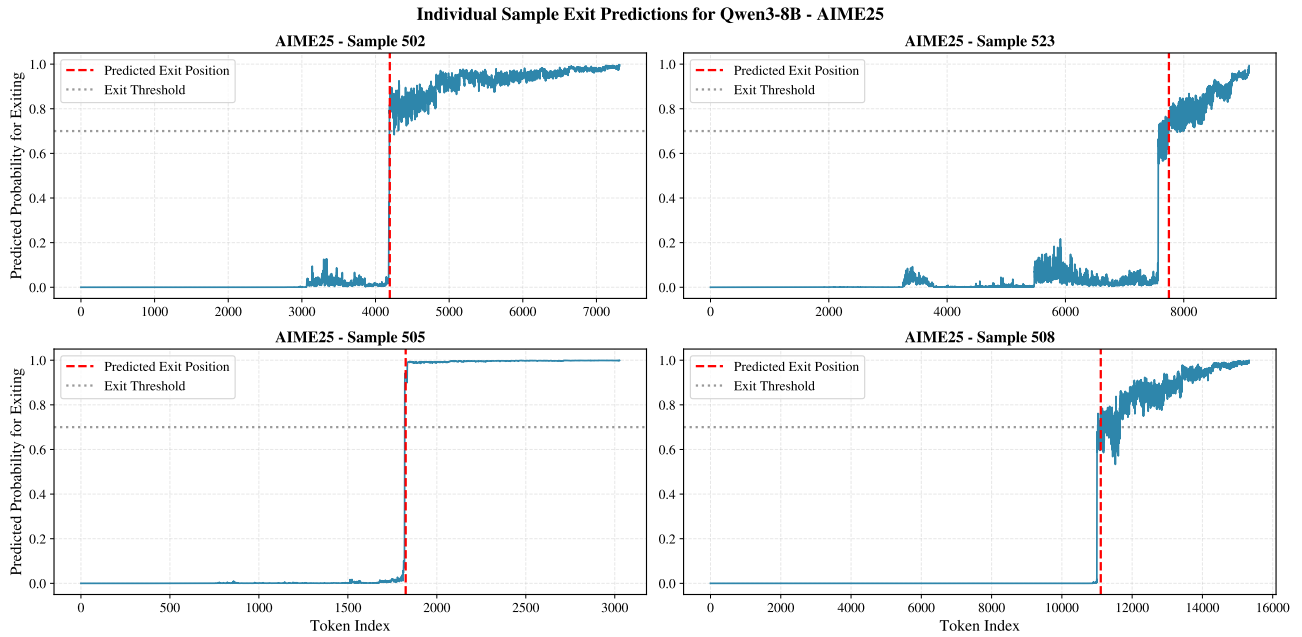


Figure 21. **Predicted Probabilities for AIME25.** TERMINATOR’s predicted probability stream for early-exiting on four randomly chosen samples from AIME25.

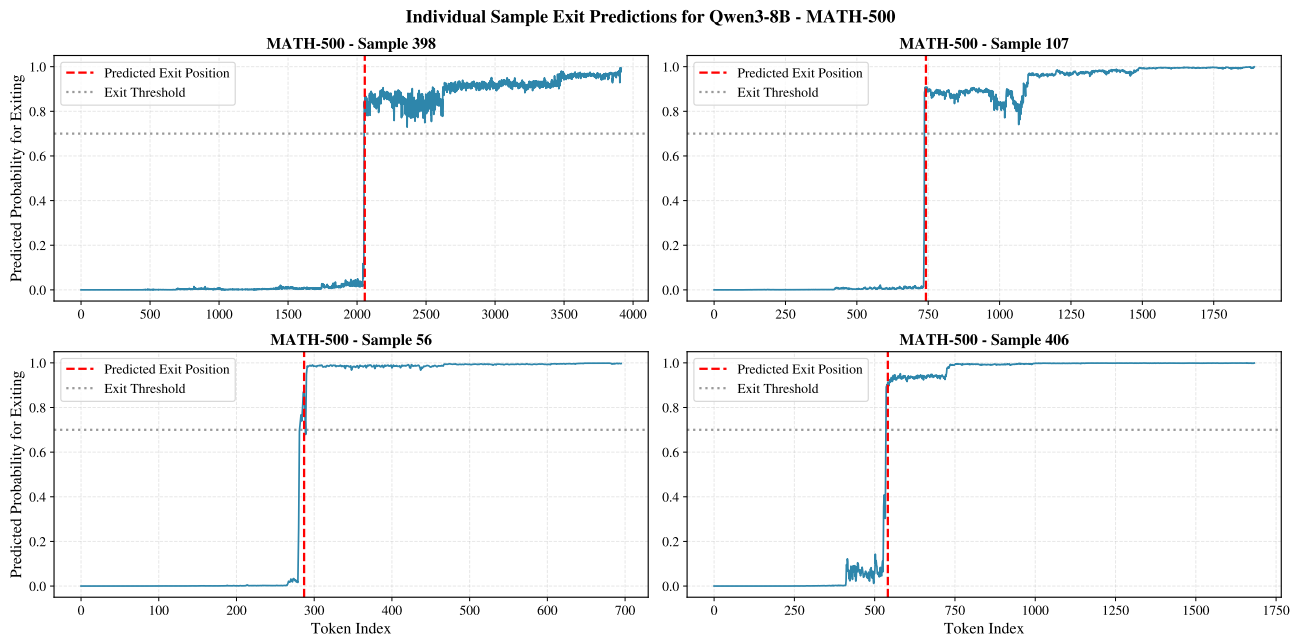


Figure 22. **Predicted Probabilities for MATH-500.** TERMINATOR’s predicted probability stream for early-exiting on four randomly chosen samples from MATH-500.

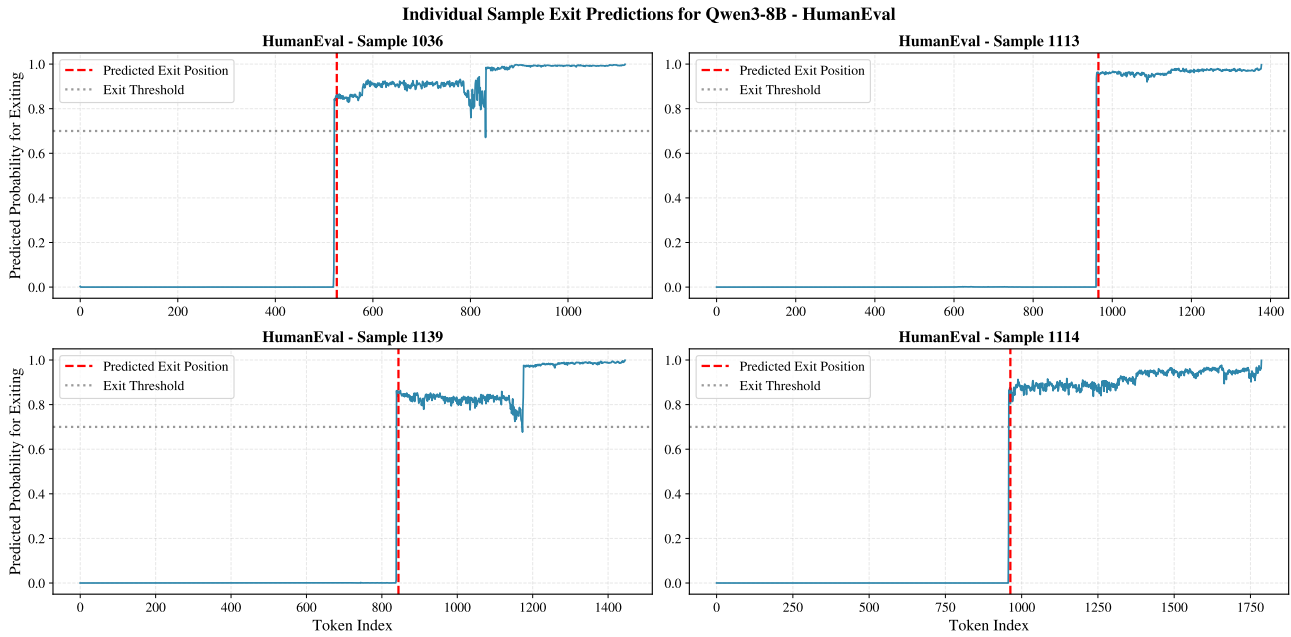


Figure 23. **Predicted Probabilities for HumanEval.** TERMINATOR’s predicted probability stream for early-exiting on four randomly chosen samples from HumanEval.

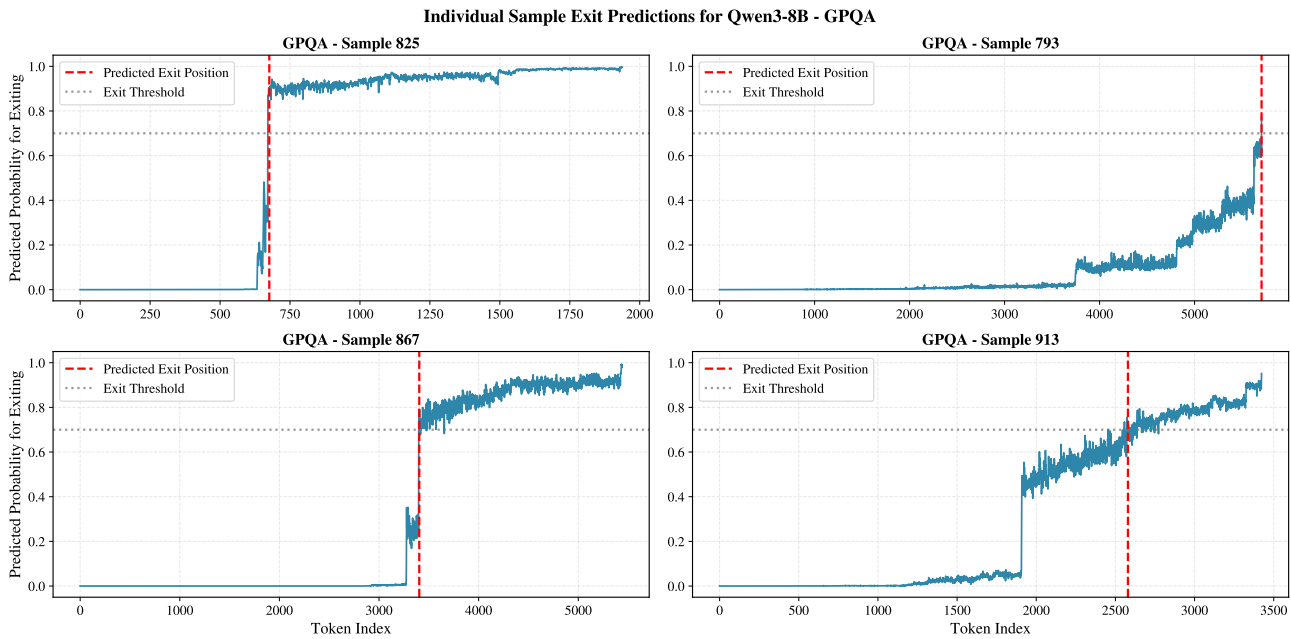


Figure 24. **Predicted Probabilities for GPQA.** TERMINATOR’s predicted probability stream for early-exiting on four randomly chosen samples from GPQA.

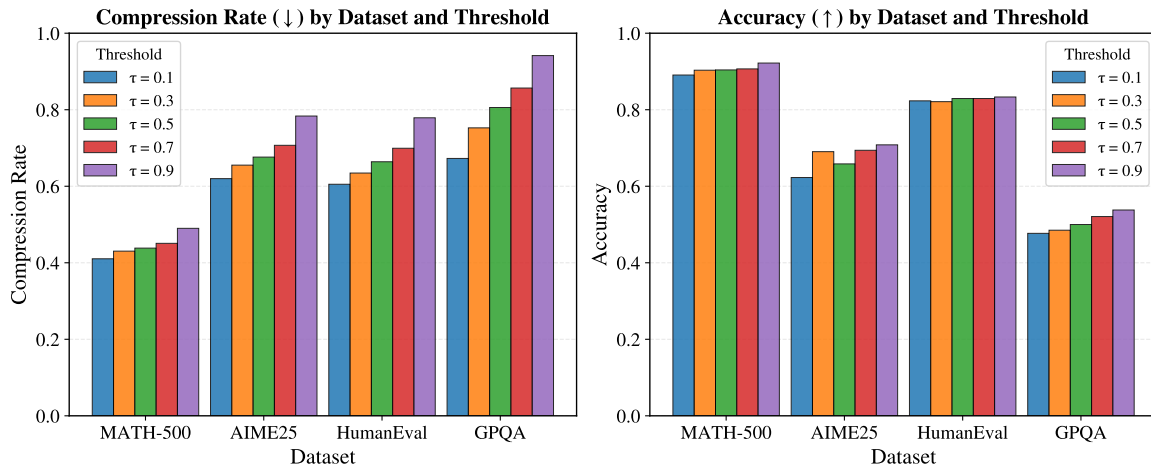


Figure 25. **Changing the Predictive Threshold.** The effect of changing the threshold of predicting 0 or 1 is altered from 0.1 to 0.9. Notably, the compression rate exhibits the largest change from $\tau = 0.1$ to $\tau = 0.9$ for all datasets, compared to the change in accuracy. In particular, some datasets, like MATH-500 and HumanEval, exhibit very little performance drop.

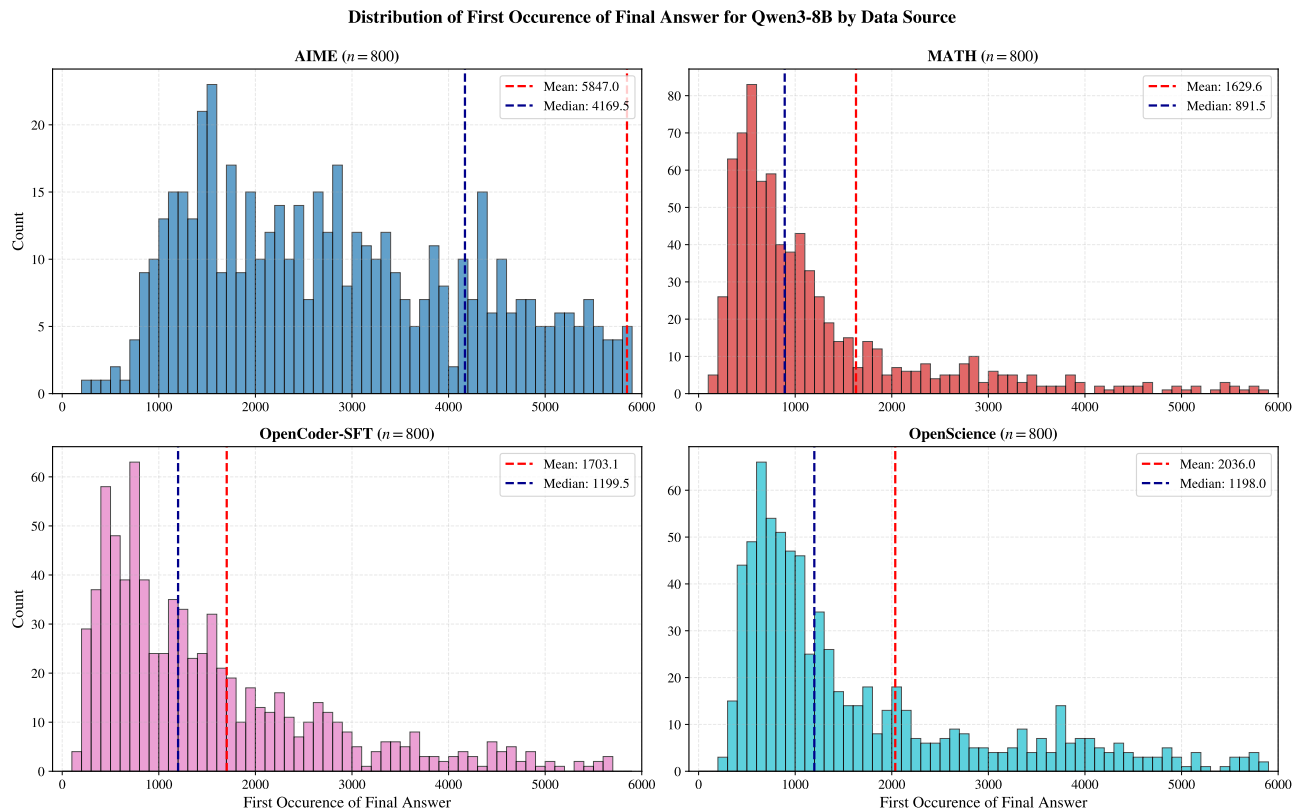


Figure 26. **First Answer Occurrence Histogram.** A histogram of the first occurrence of the final answer for each data source used in our training dataset is shown.

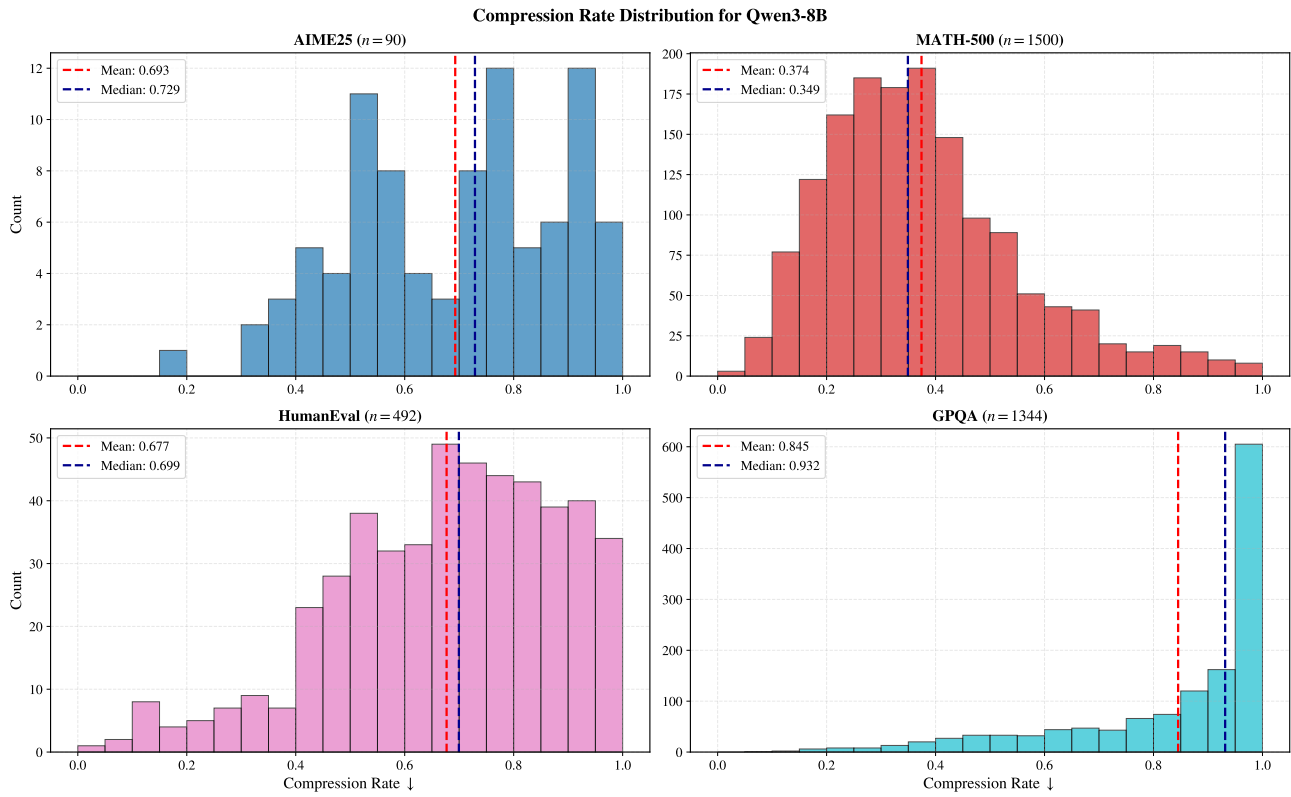


Figure 27. **Compression Ratio Histograms for TERMINATOR.** Each histogram shows the frequency of an achieved compression rate when early-exiting with TERMINATOR. ↓ indicates that a lower compression rate is better, as it results in more tokens saved with our method. Three CoTs are sampled per data source.

MATH-500, sample 77

— Early exiting position

True: 4 | Pred: 4

... a $\{ m \cdot n \}$ \$. Applying that here , the right side becomes : $2^8 = 2^{\{ 2 \times \}}$ So now both sides have the same base , which is 2 . If the bases are equal and the expressions are equal , then their exponents must be equal as well . That means : $8 = 2 \times$ To solve for x , divide both sides by 2 : $x = \frac{8}{2} = 4$ Wait , let me check if that makes sense . If $x = 4$, then 4^4 should equal 2^8 . Let me compute both : $4^4 = 4 \times 4 \times 4 \times 4 = 16 \times 16 = 256$ $2^8 = 2 \times 2 = 256$ Yes , both equal 256 . So that checks ...



Figure 28. Predicted Probabilities for MATH-500. TERMINATOR’s predicted probabilities for early-exit on a randomly chosen sample from MATH-500. The beginning and the end are truncated for better visibility.

MATH-500, sample 195

— Early exiting position

True: 24 | Pred: 24

... compute $p(4)$. Plugging in $x = 4$: $p(4) = (4 - 1)(4 - 2)(4 - 3)(4 - r) = (3)(2)(1)(4 - r) = 3 * 2 * 1 * (4 - r) = 6 * (4 - r) = 24 - 6r$. Therefore, $p(0) + p(4) = 6r + 24 - 6r = 24$. Wait, the **terms** cancel out? That's interesting. So regardless of the value of r , $p(0) + p(4)$ is 24? But how is that possible? How come we don't need to know the fourth root? Is there something wrong here? Let me check my calculations again. For $p(0)$: $(0 - 1) = -1$, $(0 - 2) = -2$, $(0 - 3) = -3$, $(0 - r) = -r$. Multiply them: (-

...



Figure 29. Predicted Probabilities for MATH-500. TERMINATOR’s predicted probabilities for early-exit on a randomly chosen sample from MATH-500. The beginning and the end are truncated for better visibility.

AIME-2025, sample 508

— Early exiting position

True: 62 | Pred: 50

... - \hat{a} | 4 1)/ 6 is not the correct y -coordinate . Therefore
 , this suggests that my initial calculation is correct , and the
 answer is $(-3 - \hat{a} | 4 1)/ 6$, which is in the form $(a -$
 $\hat{a} | b)/ c$ if we allow a to be negative , but the problem
 specifies a , b , c are positive integers . This is a contradiction
 , indicating a possible error in the problem or my solution . However
 , since the problem is from a competition , it 's more likely that
 I made a mistake . Let me revisit the quart ic equation . Earlier ,
 after substit uting $t = x \hat{a} | 3$, we had the quart ic equation t
 $\wedge 4 - 2 t \hat{A}^3 - 2 5 t \hat{A}^2 + 1 8 t + 1 2 0 =$
 0 , which fact ored into $(t \hat{A}^2 + t - 1 0)(t \hat{A}^2 - 3 t$
 $- 1 2) = 0$. Let me double -check this factor ization . Multiply
 $(t \hat{A}^2 + t - 1 0)($...



Figure 30. Predicted Probabilities for AIME25. TERMINATOR’s predicted probabilities for early-exit on a randomly chosen sample from AIME-2025. The beginning and the end are truncated for better visibility.

AIME-2025, sample 517

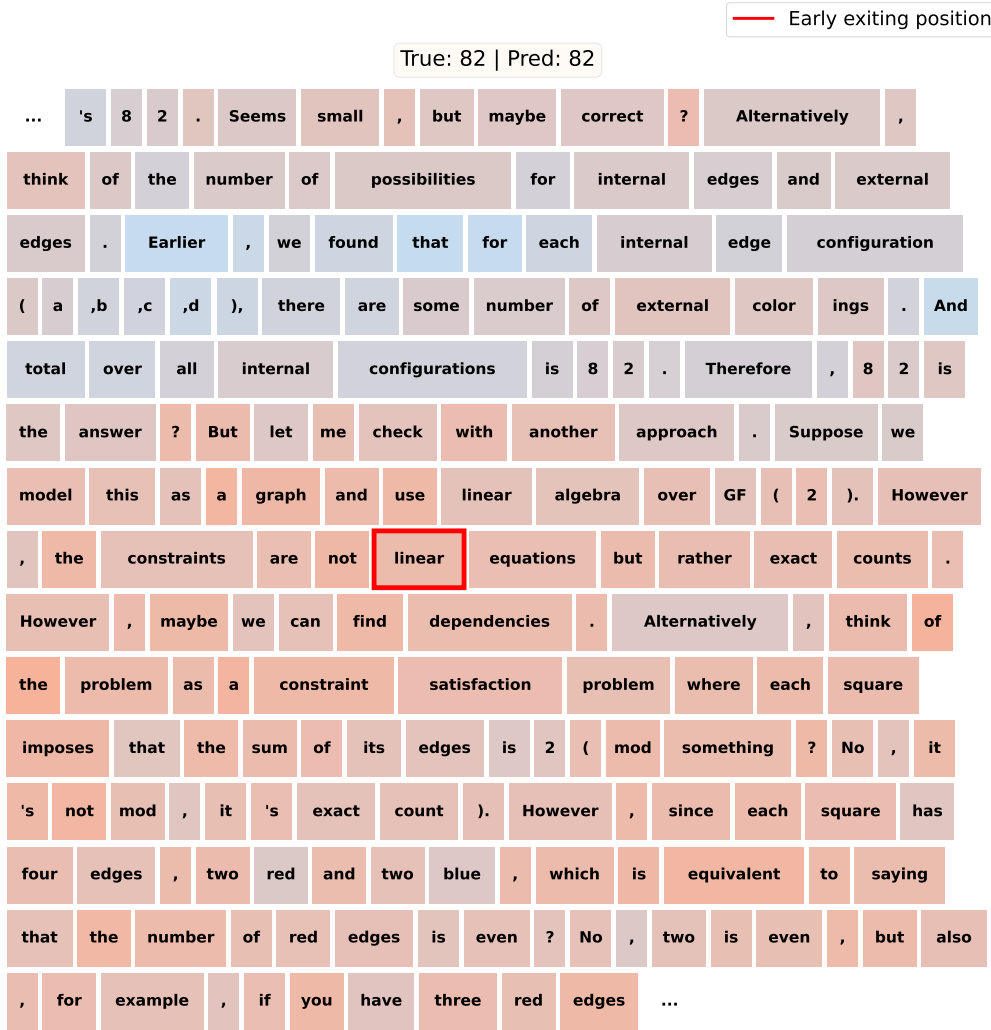


Figure 31. **Predicted Probabilities for AIME25.** TERMINATOR’s predicted probabilities for early-exit on a randomly chosen sample from AIME-2025. The beginning and the end are truncated for better visibility.